

Thesis for the degree of Doctor of Engineering

**Pure, Hybrid and Polymerized
Ionic Liquid Based Electrolytes
For High Temperature
Lithium-Ion Battery Application**

Manfred Kerner



CHALMERS

Department of Physics
Chalmers University of Technology
Gothenburg, Sweden 2017

Pure, Hybrid and Polymerized Ionic Liquid Based Electrolytes
For High Temperature Lithium-Ion Battery Application
Manfred Kerner

© Manfred Kerner, 2017
ISBN: 978-91-7597-655-6
Doktorsavhandlingar vid Chalmers tekniska högskola
Ny serie nr: 4336
ISSN 0346-718X

Department of Physics
Chalmers University of Technology
SE-41296 Gothenburg
Sweden

Cover:
Cylindrical LIB with an artistic representation of its electrolyte
© Muhammad E. Abdelhamid, 2017

Printed at Chalmers Reproservice
Gothenburg, Sweden 2017

Pure, Hybrid and Polymerized Ionic Liquid Based Electrolytes For High Temperature Lithium-Ion Battery Application

Manfred Kerner
Department of Physics
Chalmers University of Technology
SE-41296 Gothenburg, Sweden

Abstract

Today, lithium-ion batteries (LIBs) are ubiquitous in mobile phones, laptops, and other portable devices. Additionally, LIBs are becoming more and more popular for powering hybrid and electric vehicles. The research community strives to further improve the LIBs to increase electric driving distance and efficiency of both hybrid and fully electric vehicles. Conventional LIBs need to be strictly temperature controlled, most often cooled, to *ca.* 30°C, to ensure an acceptable and predictable life-time. Increasing the thermal stability and hence making possible operating temperatures of up to *ca.* 100°C would enable a merging of the cooling systems of the LIB and the power electronics – resulting in an overall reduced system complexity, saved mass, and a higher energy efficiency.

All components of the LIB must be thermally stable to deliver the targeted performance and life-time. The electrolytes of conventional LIBs all contain organic solvents and lithium salts, the former flammable with high vapour pressures and the latter meta-stable at room temperature and unstable at temperatures above 60°C. Thus more stable solvents and salts are needed to improve the inherent safety of the electrolyte – especially if aiming at elevated operating temperature applications.

In this thesis procedures to investigate electrolytes for viability in HT-LIBs are demonstrated by investigating novel high-temperature LIB electrolyte alternatives primarily in the form of pure, hybrid and polymerized ionic liquid based systems. For several of these, physico-chemical properties such as viscosity, thermal stability, flammability and electrochemical stability window have been assessed and correlated with molecular level interactions, and furthermore a detailed characterization of several commercial sources of an often used electrolyte Li-salt has been performed.

Keywords: lithium-ion battery, ionic liquid, electrolyte, polymer, high-temperature stability, LiFSI, EMITFSI, EMIFSI, Pip₁₄TFSI, Pyr₁₃TFSI

List of Publications

This thesis is based on the work contained in the following papers:

I. Thermal stability and decomposition of lithium bis(fluorosulfonyl)imide (LiFSI) salts

Manfred Kerner, Nareerat Plylahan, Johan Scheers, and Patrik Johansson
RSC Adv., 2016, **6**, 23327-23334.

II. Ionic liquid based lithium battery electrolytes: Fundamental benefits of utilizing both TFSI and FSI anions?

Manfred Kerner, Nareerat Plylahan, Johan Scheers, and Patrik Johansson
Phys. Chem. Chem. Phys., 2015, **17**, 19569-19581.

III. Elevated temperature lithium-ion batteries containing SnO₂ electrodes and LiTFSI-Pip₁₄TFSI ionic liquid electrolyte

Solveig Böhme, Manfred Kerner, Johan Scheers, Patrik Johansson, Kristina Edström and Leif Nyholm
J. Electrochem. Soc., 2017, **164**, A701-A708.

IV. Ionic liquid and hybrid ionic liquid/organic electrolytes for high temperature lithium-ion battery application

Nareerat Plylahan, Manfred Kerner, Du-Hyun Lim, Aleksandar Matic and Patrik Johansson
Electrochim. Acta, 2016, **216**, 24-34.

V. Pyrrolidinium FSI and TFSI based polymerized ionic liquids as electrolytes for high temperature lithium-ion batteries

Manfred Kerner and Patrik Johansson
In manuscript

VI. Towards more thermally stable Li-ion battery electrolytes with salts and solvents sharing nitrile functionality

Manfred Kerner, Du-Hyun Lim, Steffen Jeschke, Tomas Rydholm, Jou-Hyeon Ahn and Johan Scheers
J. Power Sources, 2016, **332**, 204-212.

Contribution Report

I. I performed all the measurements and data analysis – with the exception of the battery cycling. I was the main author of the manuscript.

II. I performed all the measurements and data analysis – with the exception of the LSV measurements and simulation of Raman spectra. I was the main author of the paper.

III. I performed the DSC, TGA, viscosity and conductivity measurements, analysed the respective data and wrote the respective parts of the manuscript.

IV. I performed the viscosity and density measurements and partly the battery cycling, analysed these data and wrote these parts of the manuscript.

V. I performed all the measurements and data analysis. I was the main author of the paper.

VI. I analysed the data – with the exception of the modelling data. I was the main author of the manuscript.

Table of Contents

Abstract	III
List of Publications	IV
Contribution Report	V
List of Figures	VIII
List of Acronyms	IX
1 Introduction	1
2 Batteries	5
2.1 Operating Principles	5
2.2 Lithium-ion Batteries (LIBs)	7
2.2.1 High Temperature LIBs	8
2.3 Electrodes	9
2.3.1 Anodes	9
2.3.2 Cathodes	10
2.4 Electrolytes	12
2.4.1 Conventional Electrolytes for LIBs	12
2.5 Electrode/Electrolyte	13
2.5.1 Solid Electrolyte Interphase (SEI)	13
2.5.2 Solid Permeable Interface (SPI)	14
3 From Li-salts to Polymerized Ionic Liquids (PILs)	15
3.1 Components	15
3.1.1 Lithium Salts	15
3.1.2 Organic Solvents	17
3.1.3 Ionic Liquids (ILs)	19
3.1.4 Polymerized Ionic Liquids	20
3.2 Electrolytes	22
3.2.1 IL Based Electrolytes	22
3.2.2 Hybrid Electrolytes	24
3.2.3 PIL Based Electrolytes	26
4 Experimental Techniques	29
4.1 Thermal Analysis Methods	29
4.1.1 Differential Scanning Calorimetry	29
4.1.2 Thermogravimetric Analysis	30
4.2 Dielectric Spectroscopy	32
4.3 Vibrational Spectroscopy	35
4.3.1 IR Spectroscopy	36
4.3.2 Raman Spectroscopy	37
4.4 Electrochemical Techniques	39

4.4.1	Linear Sweep Voltammetry	39
4.4.2	Impedance Spectroscopy	40
4.4.3	Chronopotentiometry	41
5	Summary of Appended Papers.....	43
5.1	Paper I.....	43
5.2	Paper II	44
5.3	Paper III	45
5.4	Paper IV	46
5.5	Paper V	47
5.6	Paper VI.....	49
6	Conclusions and Outlook.....	51
	Acknowledgements.....	52
	References.....	53

List of Figures

Figure 1: Energy consumption, GHG emissions (a) and xEV sales (b) [4–6].....	1
Figure 2: GHG emissions by sector in the EU, data from 2015 [11].....	2
Figure 3: The main components of an electrochemical cell and a 3S2P battery pack...6	
Figure 4: LIB with graphite anode, SEI, IL _{el} , and LiCoO ₂ cathode.	7
Figure 5: Electrodes/electrolytes energy levels for a thermodynamically (a) and kinetically (b) stable electrolyte.....	13
Figure 6: Increase in complexity from Li-salt to PIL based electrolytes.....	15
Figure 7: Structures of common cyclic and linear organic solvents.....	18
Figure 8: Structures of cations and anions of some ILs.....	19
Figure 9: Cationic IL monomers for PILs.....	21
Figure 10: Walden plot with IL classification.	23
Figure 11: Schematic illustration of the DSC measurement chamber.....	29
Figure 12: Typical DSC heating trace of an IL _{el}	30
Figure 13: TGA coupled with FT-IR spectrometer.	31
Figure 14: TGA data analysis by different methods.....	32
Figure 15: Physical origins of sample responses to electric field.....	34
Figure 16: Dielectric spectroscopy measurement cell set-up.	34
Figure 17: Absorption of photons by the transition of vibrational states.	36
Figure 18: Vibrational transitions during spectroscopic measurements.....	37
Figure 19: Raman spectrum of Li _{0.2} EMI _{0.8} TFSI with band assignments.	38
Figure 20: Electrochemical test cell and a typical voltammogram.....	39
Figure 21: Equivalent circuit (A) and corresponding Nyquist plot of a PIL _{el} (B).	40
Figure 22: Rate capabilities of an LFP electrode using a PIL _{el} [V].....	41
Figure 23: Dynamic TGA results and Raman spectra of three LiFSI salts.	43
Figure 24: Thermal stability of an IL, an electrolyte, and ESWs of all electrolytes. ..	44
Figure 25: Long-term thermal stability and ionic conductivities of Pip ₁₄ TFSI and its electrolyte.....	45
Figure 26: Viscosities and charge/discharge capacities of the electrolytes.	46
Figure 27: Cycling performance for Li PIL _{el} LFP cells at varying C-rates.	47
Figure 28: a) Discharge capacities for Li LFP cells and b) TGA FT-IR spectra.	49

List of Acronyms

ADN	Adiponitrile
CE	Counter electrode
DMAc	Dimethyl acetamide
DMC	Dimethyl carbonate
DSC	Differential scanning calorimetry
EC	Ethylene carbonate
EMI	1-ethyl-3-methyl-imidazolium
EMC	Ethyl methyl carbonate
ESW	Electrochemical stability window
EV	Electric vehicle
FP	Flash point
FSI	Bis(fluorosulfonyl)imide
FTFSI	(Fluorosulfonyl) (trifluoromethanesulfonyl)imide
FT-IR	Fourier transform infrared
GHG	Greenhouse gas
HEV	Hybrid electric vehicle
HF	Hydrofluoric acid
HOMO	Highest occupied molecular orbital
HT-LIB	High-temperature LIB
IL	Ionic liquid
IL _{el}	Ionic liquid based electrolyte
LIB	Lithium-ion battery
LiBOB	Lithium bis(oxalato)borate
LFP	Lithium iron phosphate
LTO	Lithium-titanate
LUMO	lowest unoccupied molecular orbital
MS	Mass spectrometer
M _w	Molecular weight
NiCd	Nickel-cadmium
NiMH	Nickel-metal-hydride
OCV	Open circuit voltage
PC	Propylene carbonate
PDDA	Poly(diallyldimethylammonium)
PIL	Polymerized ionic liquid
PIL _{el}	Polymerized ionic liquid based electrolyte
Pip	Piperidinium
Pyr	Pyrrolidinium
RE	Reference electrode
SEI	Solid electrolyte interphase
SHE	Standard hydrogen electrode
SL	Sulfolane
SLI	Starting, lighting, ignition
SPI	Solid permeable interface
TFSI	Bis(trifluoromethanesulfonyl)imide
TGA	Thermogravimetric analysis
VC	Vinyl carbonate
WE	Working electrode

1 Introduction

Since the dawn of the industrial age and the invention of the fossil fuel powered steam-engine, the energy consumption of the world and the emission of greenhouse gases (GHGs) have continuously and dramatically increased (Figure 1a). Merely 250 years ago, climate change was neither known of nor yet man-made. However, there is now a common consensus among scientists that climate change is a real and substantial threat to humanity [1]. This threat has been tackled by almost all countries world-wide with the signing of the *Paris Agreement* in 2015.¹ This agreement unites countries in striving to reduce the emission of GHGs in order to prevent a global warming of $\geq 2^\circ\text{C}$ in comparison to preindustrial times (< 1750) [2]. To be able to successfully fulfil this endeavour, humanity needs to abandon or drastically reduce fossil fuel consumption. This can partly be done by shifting electrical energy generation from fossil fuels to renewable energies, *e.g.* solar cells, wind, *etc.* However, other factors need to be considered as well. The transportation sector is responsible for a large portion of the total GHG emissions (Figure 2). Especially heavy-duty trucks consume a large amount of fossil fuels and have a larger share of GHG emissions compared to light-duty vehicles [3]. In order to reduce fossil fuel consumption and hence the emission of GHGs from the transportation sector, the electrification and accessibility of electrified vehicles needs to continue to advance (Figure 1b). Both can be fostered by advancements in battery technology.

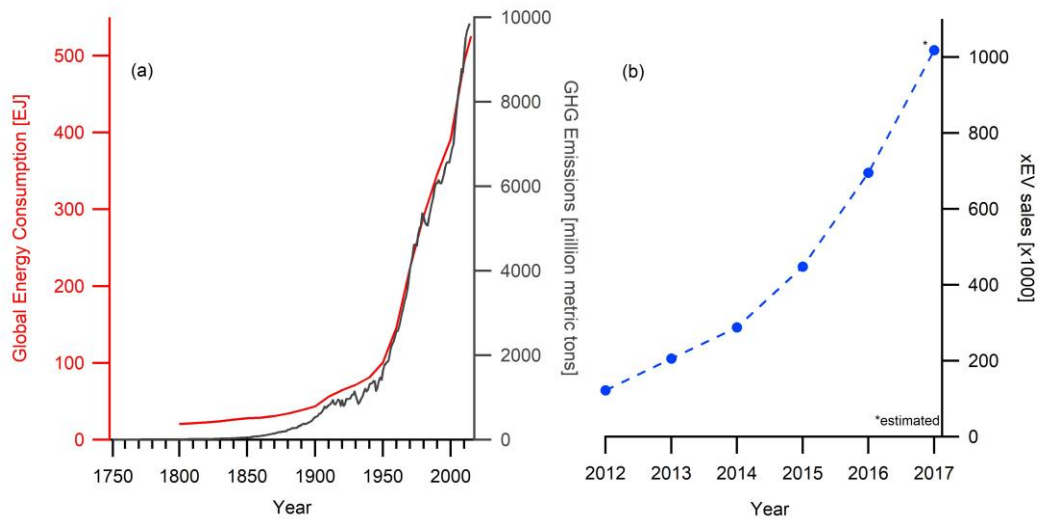


Figure 1: Energy consumption, GHG emissions (a) and xEV sales (b) [4–6].

The first appearance of batteries in “car-like” vehicles dates back to the beginning of the 19th Century [7]. With the advance of chemistry, battery technologies have improved (Table 1). This has resulted in a shift in battery technology from lead-acid batteries of the very first fully electric vehicles (EV) to the nickel metal hydride batteries (NiMH) employed in one of the first modern hybrid electric vehicles (HEV) -

¹ Despite that USA announced to withdraw from the Paris Agreement in June 2017.

the Toyota Prius in 1997. Today, lithium-ion batteries (LIBs) are becoming more and more popular for the xEV market, with improved specific energies, capacities and cycle-lives. As a result of this shift, driving ranges of up to 500 km have recently been made possible and accessible to a larger market [8]. The research community further strives to improve the LIB in order to increase distance and efficiency, while decreasing the cost of xEVs [9,10].

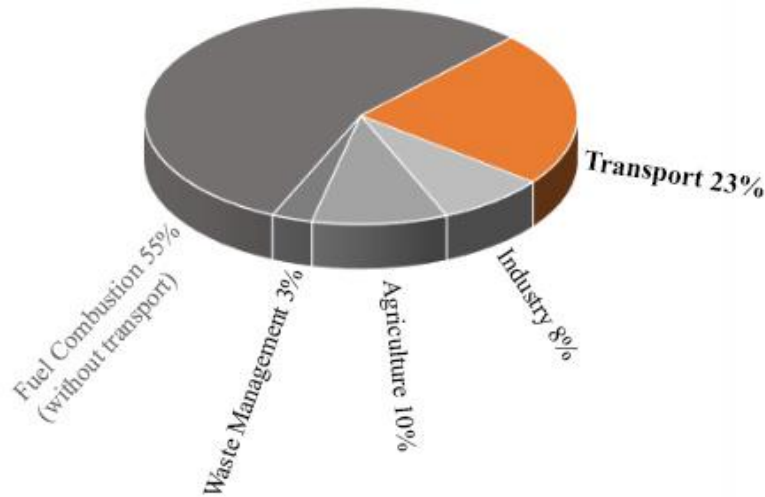


Figure 2: GHG emissions by sector in the EU, data from 2015 [11].

A sometimes, at least to the public as compared to the xEV cars, forgotten area is commercial vehicles; trucks, buses, construction equipment, *etc.* In this thesis an opportunity to increase the efficiency of hybrid-trucks is outlined by the concept of LIBs with higher operating temperatures (HT-LIBs). Today's LIBs contain several components, of which one is the ion conducting electrolyte. This electrolyte consists of a lithium salt, such as lithium hexafluorophosphate (LiPF_6), dissolved in a mixture of organic solvents, such as ethylene carbonate (EC) and dimethyl carbonate (DMC). However, these organic solvents are highly flammable and decompose at temperatures higher than 60°C . This makes them hazardous, especially when combined with the thermally unstable LiPF_6 salt [12]. The decomposition is not only dangerous due to the build-up of pressure and risk of explosion, but fluorine based salts can also lead to the evolution of hazardous gases such as hydrofluoric acid (HF) [12]. Furthermore, it has been shown that both the calendar and cycle life of LIBs are strongly dependent on the temperature. The cycle life of a LIB is reduced from > 3000 cycles to *ca.* 1600 cycles when increasing the temperature from 25 to 45°C [13]. Thus, conventional LIBs need a separate cooling system, keeping them at *ca.* 35°C , while the power electronics are cooled to *ca.* 80°C . Improving the thermal stability of the LIB electrolyte would provide an opportunity for a joint cooling system, and thereby improve the overall vehicle weight and efficiency. Furthermore, the higher working temperatures can make other electrode materials with improved power densities viable.

Table 1: Properties of some battery technologies [14,15].

Chemistry	Cell Voltage [V]	Spec. Energy [Wh/kg]	Cycle Life [#]	Power Density [W/kg]	Oper. T. [°C]
Lead-acid	2.0	30	250-500	1-200	-40 to 60
NiMH	1.2	90-110	500-1000	10-400	-20 to 65
LIB	4.0	200	1000+	1-2000	-20 to 50

To improve the safety of the electrolyte, flame-retardants can mitigate electrolyte flammability [16–18], but a more robust solution is to find more stable salts and solvents. Ionic liquid (IL) based electrolytes (IL_{el}) are promising for high-temperature applications such as the HT-LIB. ILs contain only ions and are by definition salts with melting points below 100°C and frequently liquids even at ambient temperatures. Research on ILs has flourished during the last decade [19], but no "Swiss Army Knife" IL is likely to be found. However, it should be possible to find an IL_{el} with all the properties (high thermal stability, wide electrochemical stability window, high ionic conductivity, *etc.*) needed for an HT-LIB [20–22]. In spite of their advantages, ILs have comparatively high viscosities, and ionic conductivities are not only arising from the Li⁺, suggesting that modified concepts such as IL/organic solvent hybrid electrolytes may be needed.

The addition of an organic solvent to an IL can improve the transport properties of the electrolyte without dramatically impairing its safety properties as shown by Montanino *et al.* for a LiTFSI in Pyr₁₃TFSI/EC/DEC electrolyte [23]. In **paper IV**, we performed promising half-cell cycling of Li||lithium iron phosphate (LFP) cells with hybrid electrolytes, that show capacities of 150-160 mAh/g at 1 C and 80°C. Another alternative is to combine the advantages of ILs and polymer, creating poly-ILs (polymerized ILs, PILs) by polymerizing IL monomers and interconnecting them covalently to create a polymer-backbone [24]. These PILs have high thermal stabilities but only moderate ionic conductivities [25]. The application of ternary electrolytes where a Li-salt, an IL and a PIL are combined (ion-gels) lead to increased ionic conductivities with maintained high thermal stabilities. In **paper V**, we have shown that this concept leads to stable cycling of Li||LFP half-cells for 100 cycles at 0.5 C and 80°C. A further alternative concept for safer and more thermally stable LIBs is the utilisation of nitrile based salts and solvents, which we have investigated in **paper VI**.

This thesis starts by introducing the basic operation principles of batteries in general and the LIB and electrolytes in particular, before moving on to the materials needed to create IL_{el}. Various HT-LIB electrolyte concepts: Pure, hybrid and polymerized IL, and nitrile based electrolytes are then scrutinized for their physico-chemical properties. Some of the tested electrolytes have also had their electrochemical performance assessed, with special emphasis on the thermal stability of the materials used, including the Li-salt.

2 Batteries

Batteries are electrochemical devices that store chemical energy and transform it to electrical energy when discharged. They can be classified as either primary or secondary [14]; the former being disposed after single use, while the latter can be recharged and used again. From here onwards the term “battery” is used synonymously for a secondary/rechargeable battery.

Today’s engineers can choose from a wide variety of batteries as a power source for a diverse number of applications, including electric vehicles, stationary storage, *etc.* Every battery technology has its own unique advantages and disadvantages, making them suitable for different applications. The different properties of a few selected battery concepts are listed in Table 1. The lead-acid concept is well established as a starting-lighting-ignition (SLI) battery in vehicles [26]. This is due to its high power density of 200 W/kg, the wide operating temperature of -40-60°C and its low price [14]. Nickel-metal-hydride (NiMH) batteries are used in areas that require both high power density and high specific energy (*e.g.* cameras, power tools) and have been used in the first generations of HEVs. The slightly improved specific energy of the NiMH battery compared to the nickel-cadmium (NiCd) battery technology makes it slightly superior². In the present day LIBs have the highest specific and volumetric energies of 200 Wh/kg and 570 Wh/L, respectively, as well as long cycle life of more than 1000 charge-discharge cycles and very high cell voltages of *ca.* 4 V [15,27]. This makes them ideal for devices where low weight and volume is a crucial factor, such as mobile phones, tablets, power tools, and xEVs.

2.1 Operating Principles

The electrochemical cell is the basic unit of a battery and consists of two electrodes and an electrolyte (Figure 3). Redox reactions take place at the electrodes when the battery is operated: oxidation at the anode and reduction at the cathode when discharged [14]. These reactions are reversed when the cell is charged. The resulting electrical current flowing from anode to cathode needs to be charge-compensated by ion transport through the electrolyte. In case of liquid electrolytes, a separator is needed, to prevent the electrodes from physical contact and the battery from short-circuiting. Commonly, a microporous polyolefin (*e.g.* polyethylene (PE), polypropylene (PP)) separator of 16-40 μm is used, which keeps its functionality up to its T_m (PE:135°C and PP:155°C), while glass microfiber composite separator show even a higher thermal stability of 200°C [14,28]. The three basic components of the electrochemical cell are necessary for the battery to function, but usually only the electrodes store and deliver energy – which is why these are dubbed “active materials”. Electrode materials are introduced and discussed in sub-chapter 2.3.

²NiCd batteries have been banned for sale in the EU, because of the toxic cadmium, but are still used in applications where no alternatives exist.

A battery is made of at least one electrochemical cell and other components such as current collectors. The current collectors ensure an efficient electronic transport between the electrodes by their high electrical conductivity (commonly made of copper or aluminium). Additionally, they provide mechanical stability to the electrode material and are electrochemically stable to not influence the electrode processes [29]. Single battery cells are connected to one another to reach desired voltages (series connection) and/or desired energy and power (parallel connection). The resulting battery module can be connected to other modules to further increase voltage, energy, and power. In EVs, a voltage power supply of *ca.* 400 V provides high efficiency as well as lighter vehicles due to the decreased weight by thinner cables [30]. Also, for a series connection, the failure of a single cell leads to complete module failure, while for a parallel connection a cell failure only decreases the functionality of the module. In practice, a combination of parallel and series connections is most commonly used and abbreviated by the number of cells in series and in parallel such as 3S2P for three cells in series in two parallel lines (Figure 3). The entity of cells and modules is called the battery pack. The 100 kWh battery pack in Tesla’s “Model S” EV for example, is made out of 8256 small, cylindrical, 18650 (18 mm diameter and 65.0 mm length) single-cell batteries [31]. Furthermore, temperature sensors and other control units are built in the modules and battery pack and controlled by the battery management system (BMS). The BMS also controls the charging of the battery and recuperation during deceleration of the vehicle and the health of the battery in general [29].

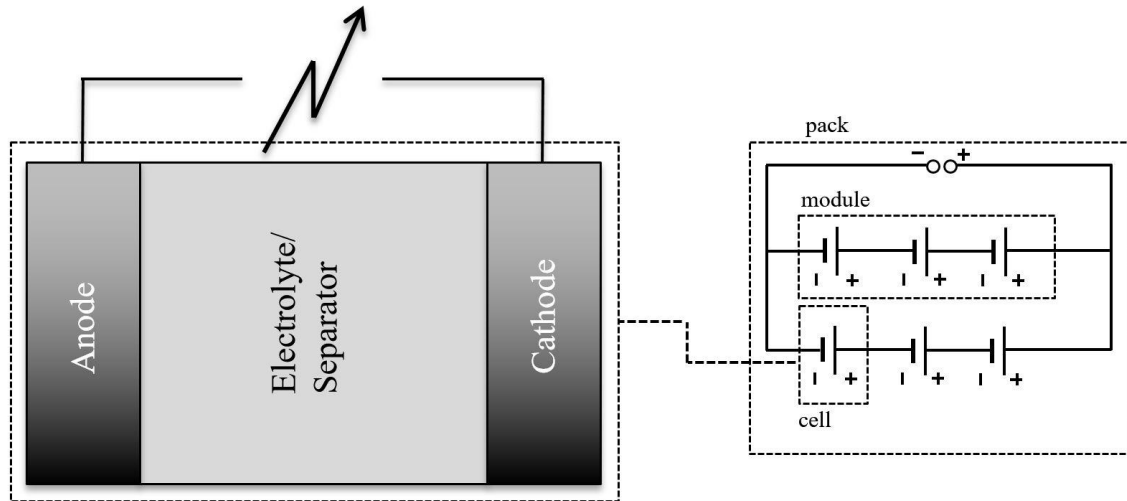


Figure 3: The main components of an electrochemical cell and a 3S2P battery pack.

Before proceeding, the most important battery properties and measures must be briefly introduced. The *output voltage* is determined by the potential difference of the half-reactions of the electrodes. LIBs have (with high cell voltages of 4 V) a large advantage over most other technologies (2 V or less, Table 1). The *specific energy* describes the amount of charge that can be extracted per kg of battery material for a certain voltage. The specific energy is with 200 Wh/kg highest for LIBs, approximately twice the energy can be extracted compared to a NiMH battery of the same weight, or equivalently, half the weight can be saved for the same output (Table 1). The *capacity*

gives information about how much current or charge can be extracted over time, or how long the battery is going to work for before the active materials are depleted. The ratio between electric charge transferred during battery charge and discharge determines the *coulombic efficiency*. The *rate capability* defines the highest current extractable from a battery. The *cycle stability* describes how the discharge capacity is reduced, *e.g.* to 80% of its initial value, with increasing cycle number. Depending on the battery technology the cycle stability varies from 250 to more than 1000 cycles with LIBs being at the upper end of this range. However, it is notable that none of the battery technologies in Table 1 have a thermal stability higher than 65°C. Creating a HT-LIB makes the already compelling LIB technology even more attractive, as to its high energy, power density and long-cycle life, the increased thermal stability would further increase the efficiency of the xEV through a simpler cooling-system (chapter 1).

2.2 Lithium-ion Batteries (LIBs)

LIBs have their origin in primary lithium metal batteries, which made use of the low atomic weight (7 g/mol) and very negative potential (-3 V vs. standard hydrogen electrode (SHE)) of lithium enabling light-weight batteries with energy densities of 250 Wh/kg [14,32]. Despite the advantages of lithium as an anode material, for safety reasons it is not commonly used in its metallic form in secondary batteries. Upon charging of the battery, metallic lithium can re-deposit on the anode in the form of dendrites, which can grow to the cathode, short-circuit the cell and lead to thermal runaway [33]. Therefore, higher specific capacities are neglected in favour of reliability, cycle stability and safety leading to the LIB.

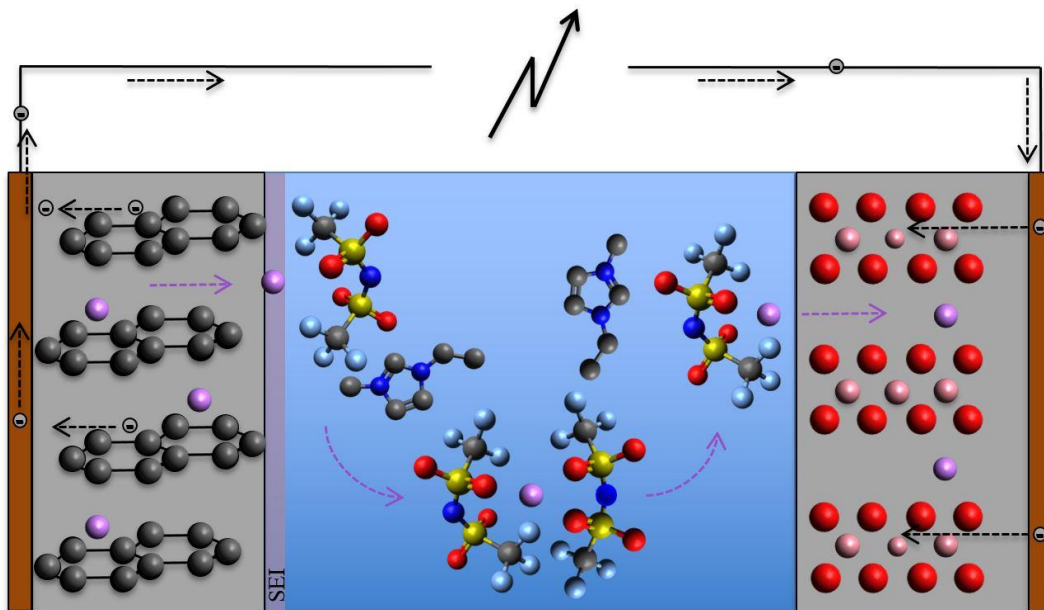


Figure 4: LIB with graphite anode, SEI, IL_{e1} , and $LiCoO_2$ cathode.

In a LIB both the anode and cathode can be intercalation materials (Latin “intercalare” = to insert, Figure 4), storing lithium in its ionic form. During charge and discharge the electrodes expand/contract only slightly as the Li^+ are intercalated or de-intercalated [34]. Based on the intercalation mechanism, LIBs are also called “rocking chair” batteries [35,36]. As an example, when graphite is used as anode material, the first cycles have lower coulombic efficiencies due to the creation of the solid electrolyte interphase (SEI) [9] (Figure 4 and sub-chapter 2.5.1). However, this SEI is one of the reasons for the long cycle life of the LIBs as it prevents further reaction of the electrode with the electrolyte and lets only the Li^+ pass through preventing graphite exfoliation induced by larger molecules [37]. Lithium is stored between the graphene layers of graphite. The lithiation process occurs in distinct insertion stages, where one model describes this by the number of empty graphene layers between two Li^+ . Upon lithiation, this number decreases from *stage IV* (every fourth layer is filled with Li^+) to *stage I* (every layer is filled with Li^+) [29]. A fully lithiated graphite contains one Li^+ for every six carbon atoms (LiC_6). More about carbons and other anode materials such as based on lithium alloying with other metals and compounds are discussed in sub-chapter 2.3.1.

2.2.1 High Temperature LIBs

Batteries with high power densities are often used for applications with a high current demand, which is accompanied by a large heat generation. LIBs have high power densities up to 2 kW/kg (Table 1) and in xEV the current is not only high, but can also be drawn for a longer period of time, increasing the temperature of the LIB. As the thermal stability of an LIB often is restricted to $\leq 50^\circ\text{C}$ (Table 1), a battery cooling system is needed [38]. One alternative is the lithium metal polymer batteries, employing a poly(ethylene oxide) based solid polymer electrolyte (SPE), that operate at $60\text{-}80^\circ\text{C}$ in the Bolloré Bluecars in Paris, but their specific energy density of 100 Wh/kg is clearly below LIBs and they demand continuous charging when not in use [39,40].

Various measures must be taken to increase the thermal stability of LIBs and create working HT-LIB. The thermal stability of the electrolyte must be improved by utilising salts and solvents with higher thermal stabilities (chapter 3). However, increasing the thermal stability of the electrolyte is not enough, also the anode and cathode materials have to withstand the higher temperatures. The reactivity of the lithiated anode towards the electrolyte sets the upper temperature limit where chain-like decomposition reactions are irreversibly triggered [41]. The addition of an additive, *e.g.* vinyl carbonate (VC), to the electrolyte can stabilize the interphase of the anode and electrolyte and increase the thermal stability. Similar problems need to be tackled on the cathode side; the main source of heat in a battery is often the reaction between the electrolyte and the delithiated cathode [41]. A small amount of dimethyl acetamide (DMAc) in the electrolyte can mitigate the reaction [42], but there is no ideal electrolyte additive to perfectly protect the electrodes at higher temperatures.

Instead of increasing the thermal stability of the electrodes used at “normal” operating temperature by modifying the electrolyte, an alternative is to use electrode materials already stable at the elevated temperatures aimed for with the HT-LIB concept. $\text{Li}_4\text{Ti}_5\text{O}_{12}$ (LTO) and chromium-rich oxidized stainless steel electrodes, $(\text{Fe}_x\text{Cr}_{1-x})\text{Cr}_2\text{O}_4$ ($0.3 < x < 1$) have been successfully tested at 60°C and 100°C , respectively [43,44]. Unfortunately, the increase in thermal stability is often accompanied by a decrease in energy density and cycle stability.

2.3 Electrodes

In the same way that there are different kinds of battery chemistries suitable for certain applications, there are also a variety of materials available which can be used as electrode materials for LIBs, resulting in LIBs with different properties. Potentials, capacities, rate capabilities, cycle life and not least the compatibility with the electrolyte can be tailored by choosing the anode and cathode electrode materials.

2.3.1 Anodes

In general, there are two types of anodes for LIBs: Intercalation and conversion materials. Intercalation materials, as shortly mentioned above, provide the host material for de-/lithiation processes, also named topotactic reactions, *i.e.* the crystal structure remains unchanged. These structures deliver high cycle-life and good capacity retention; however, they have a rather low capacity. In contrast, the conversion materials show very large capacities but have only limited capacity retention, as they are often connected to volume changes (Table 2).

Arguably, the cheapest anode materials are different types of carbons [45,46]. There are amorphous (hard and soft) and crystalline carbons (graphite). Amorphous carbons have a slightly higher delithiation potential than graphitic carbons. They also show a higher irreversible capacity retention, but because of defects and their structure being composed of monolayers, they can also provide a higher than theoretical gravimetric capacity [47]. Graphitic carbons are still the most commonly used anode materials [48]. They have a potential close to lithium metal (+0.1 V) and high cycling stability. The thermal stability of graphite has been shown to be higher than 120°C and can further be improved by increasing the carbon particle size, however, these tests were performed on lithiated graphites which were not in contact with the electrolyte [49]. Their thermal stability in contact with the electrolyte may differ.

Other types of intercalation compounds have structures in the spinel-framework. In the last decade, increased research has been performed on the spinel type anode lithium-titanate ($\text{Li}_4\text{Ti}_5\text{O}_{12}$, LTO) [50]. This material undergoes almost no volume change upon de-/intercalation (Table 2). Therefore, extremely long cycle-lives of 30000 cycles have been reported [51]. LTO's considerably higher potential of 1.6 vs. $\text{Li}^+/\text{Li}^\circ$ makes it

interesting for application with electrolytes of low reduction stability [48]. At the same time, the (for an anode) relative high potential leads to LIBs with only low output voltages [50]. LTO is very promising for HT-LIBs as it has already been tested in a battery at 60°C and the material itself at 900°C [52,53].

Table 2: Properties of anode materials for LIBs, with lithium shown as a ref.

Anode Material	Gravimetric Discharge Cap. [mAh/g]	Potential vs. $\text{Li}^+/\text{Li}^\circ$ [V]	Volume change [%]	Promising for HT-LIB?	References
Li	3860	0.0	~0	?	[32]
Graphite	372	0.1	10	?	[48]
LTO	175	1.6	0.2	Yes	[48,50]
Si	4200	0.4	270	Yes	[48,54]
C/Si	1250	0.4	270	?	[55]
Sn	790	0.7	255	Yes	[48,56]

Silicon (Si) based anode materials have a high theoretical discharge capacity of 4200 mAh/g, in addition to flat discharge profiles [57]. Unfortunately the high capacity comes along with a volume change of up to 400% [54]. This large volume expansion causes stress, leading to cracking and pulverization of the Si-particles and their SEI (sub-chapter 2.5.1), resulting in a rapid capacity degradation [57]. The combination of Si based particles with carbonaceous material, by encapsulating [58], layering [59], and binding [60] improves the electronic conductivity and quality of the SEI layer. Altogether resulting in a stable battery cycling performance of 100 cycles, delivering a capacity of 1200 mAh/g at a current density of 0.5 A/g [55].

Other promising graphite substitutes with a volumetric capacity of 2020 mAh/cm³ and low potential of 0.7 V vs. $\text{Li}^+/\text{Li}^\circ$ are tin (Sn) based anodes [56]. Similar to Si, Sn based electrodes are prone to volumetric expansion upon charge/discharge, sharing the same disadvantages of fast capacity fade and pulverisation of the Sn particles. In **paper III**, we investigated Sn based electrodes with IL_{el} at 80°C and reported comparable battery performance to commercial organic based electrolytes at RT. Both Si and Sn based anodes are promising for HT-LIBs, as they both have their origin in cells working at *ca.* 400°C [56].

2.3.2 Cathodes

Classified by the dimension of their Li-intercalation paths, there are three major types of cathode materials. These three types are: 1D olivine structured LiMPO_4 (M = Fe, Mn, Ni, Co), 2D layered, transition-metal oxide LiMO_2 (M = Co, Cr, Mn, Ni, or V) [61,62] and 3D spinel materials such as LiM_2O_4 (M = Mn, Co, Ni) are the most popular cathode materials for LIBs [63,64].

LiFePO₄ (LFP) electrodes have rather low potentials as cathode materials for LIBs (Table 3). This is a disadvantage with respect to cell output voltage and energy density, on the other hand it contributes to the very good cycle stability and safety, as electrolyte solvents do not produce oxygen under abuse condition when LFP is used [65]. Other disadvantages are the low electronic and Li⁺ conduction in LFP due to the 1D intercalation path. However, a capacity of 160 mAh/g together with its environmental friendliness, good cycling stability and low cost make it a popular cathode material. In LFP, the P-O covalent bond is very strong giving LFP a high thermal stability of $\geq 200^{\circ}\text{C}$ [66].

The 2D layered structure of LiCO₂ (LCO) provides good cycle stability and adequate rate capabilities. The theoretical capacity of LCO can only partly be used, because its structure becomes chemically unstable when too much Li is removed from it, leading to irreversible degradation and capacity fading. Furthermore, it has been shown that LCO is the least thermally stable of all commercialized common cathode materials. However, the onset temperature for its self-heating rate is above 160°C [67], which would be enough to enable HT-LIBs. LiNiO₂ and LiMnO₂ are both more stable, especially when doped by Co. This enables higher capacities up to 180 mAh/g for LiNiO₂. Furthermore, the doping of Al, Mg, Ca or Ba increases cycling stability and improves the electrode materials' thermal stability. Disadvantages of LCO are its high cost and toxicity. The 2D layered structures which contain higher amounts of the more environmental friendly and more abundant Ni and Mn, *e.g.* LiNi_{1-x-y}Mn_xCo_yO₂ (NMC) and LiNi_{0.8}Co_{0.15}Al_{0.05}O₂ (NCA) are very popular in xEVs [27].

Table 3: Properties of common cathode materials [27,48].

Cathode Material	Specific Capacity [mAh/g]	Average V vs. Li ⁺ /Li ^o [V]	Power Density	Promising for HT-LIB?
LCO	155	3.8	Good	Yes
LFP	160	3.4	Good	Yes
NMC	160	3.7	Good	Yes
NCA	180	3.7	Good	Yes
LMO	120	4.1	Very good	No

The spinel structure of LiMn₂O₄ (LMO) has 3D Li⁺ intercalation paths and provides high rate capability and safety. It has a rather low theoretical capacity of 148 mAh/g and shows an average potential of 4.1 vs. Li⁺/Li^o [48]. It is very important not to “over-discharge” batteries with LiMn₂O₄ cathodes. This is because it induces a structural change from cubic to tetragonal symmetry (Jahn-Teller distortion), causing a large volume change and capacity fading. Furthermore, trace amounts of H⁺ lead to dissolution of Mn²⁺, which migrate and get reduced irreversibly at the anode, causing capacity fading. This dissolution is promoted by temperature and is severe for

$T \geq 50^\circ\text{C}$. Even though novel, spherical heterostructures of LiMn_2O_4 , with a layered coating and spinel core have shown to be stable for 100 cycles at 60°C [68], further research still has to be done to make it suitable for HT-LIBs.

2.4 Electrolytes

An electrolyte is a medium that contains moveable ions. It has to possess many properties (Table 4) and has to be matched with the electrode materials, current collectors and operation conditions. There are electrolytes in the form of liquids, gels, polymers, and solids.

Table 4: Important electrolyte properties.

Property	Relevance/Action
SEI formation	Protects the electrodes from degradation by reacting with the electrolyte and prevents anion intercalation.
Salt solubility	Affects the maximum possible concentration of charge carriers.
Ionic conductivity	Ensures a high mobility of charge carriers which is crucial for the power density.
Electrochemical stability window (ESW)	Determines the electrodes the electrolyte can be used with.
Wide temperature range	Increases the temperature environment the battery can be used in.
Hydrolysis stability	Improves the chemical stability and prevents HF formation.
Non-flammability	Ensures safety even in case the battery is damaged by an external hazard.
Price	Assures commercialization.

2.4.1 Conventional Electrolytes for LIBs

As mentioned above, the conventional electrolyte for LIBs is based on the LiPF_6 salt dissolved in a combination of different cyclic and linear carbonate organic solvents [69], *e.g.* EC and DMC. This electrolyte concept was proposed more than two decades ago by Tarascon *et al.* [70]. EC and DMC combine several important properties: EC has a high dielectric constant, that promotes lithium salt dissolution, and forms an efficient SEI layer on graphite [71]. However, recently, Dahn *et al.* showed EC to be only suitable for Li-ion cells operating $\leq 4.2\text{ V}$ [72]. Furthermore, the melting point, T_m , of 36°C for EC calls for usage with other solvents like DMC, which lowers both the melting point and the viscosity of the resulting electrolyte – the latter important for a high ionic conductivity. An overview of the most common organic solvents and some key properties are shown and discussed in sub-chapter 3.1.2.

The classical electrolytes for LIBs have enabled thousands of charge-discharge cycles with optimized electrode configurations [38]. However, for HT-LIBs these electrolytes need to be replaced due to their non-suitability for temperatures $\geq 50^\circ\text{C}$, especially when the lithium salt LiPF_6 is used [12] – alternatives are pure, hybrid and polymerized IL_{el} [10]. Furthermore, in **paper VI** we have investigated promising liquid nitrile based electrolytes for HT-LIBs.

2.5 Electrode/Electrolyte

With respect to electrode/electrolyte interfaces, there are two possible ways to achieve a well-functioning combination of electrodes and electrolyte. Either, the potentials of the electrodes are within the ESW of the electrolyte or the electrochemical stability is increased by an SEI or an SPI – interphases between the electrolyte and the electrode.

2.5.1 Solid Electrolyte Interphase (SEI)

The electrolyte is composed of organic solvents with molecular energy levels, whereof the highest occupied molecular orbital (HOMO) and lowest unoccupied molecular orbital (LUMO) determine their intrinsic electrochemical stabilities. If the LUMO/HOMO levels are outside of the potentials of the anode/cathode, the electrolyte and the battery is stable (Figure 5a). A higher potential of the anode than the LUMO can lead to reduction of the electrolyte [9]. An SEI is formed on the surface of the anode in case SEI forming species (*e.g.* EC) are present. This happens immediately upon contact with metallic lithium anodes, but cell cycling is necessary for uncharged (*e.g.* graphite based) anodes [73].

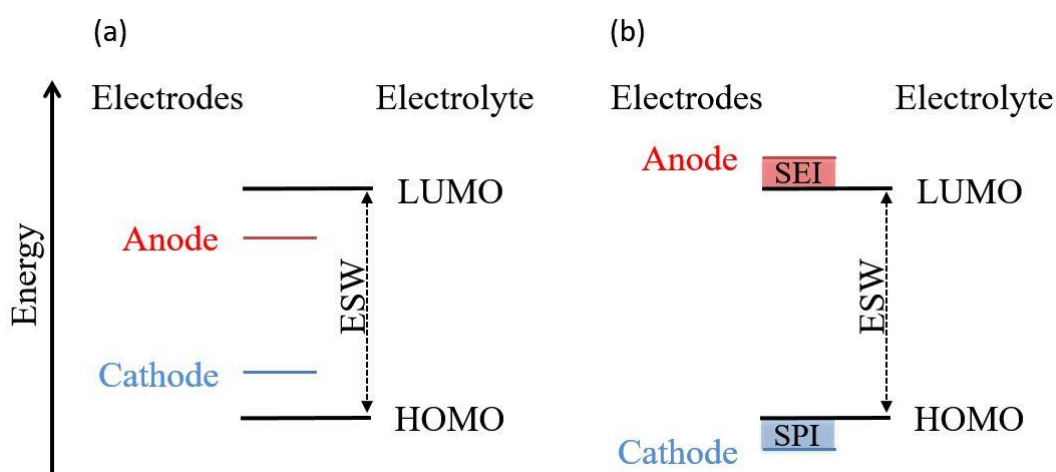


Figure 5: Electrodes/electrolytes energy levels for a thermodynamically (a) and kinetically (b) stable electrolyte.

The SEI model was proposed in 1979 by Peled and was confirmed for all alkali and alkali earth metals [74]. The SEI prevents further decomposition, but still facilitates transport of the small Li^+ during charge and discharge [75]. It is of utmost importance that the SEI is of high quality. This can be achieved by having mechanical stability and flexibility, as well as possessing a temperature expansion coefficient in the same range as the anode's. If the SEI cannot perfectly protect the anode, continuous reduction of the electrolyte will occur and increase the thickness of the SEI. A regular SEI was originally stated to be thermally stable up to 120°C [76], but a detailed XPS-study later showed its decomposition to be close to RT [77].

2.5.2 Solid Permeable Interface (SPI)

Similarly to the formation of the SEI on the anode, the SPI is formed on the surface of the cathode (Figure 5b). Here, the electrolyte is oxidized by the cathode if the HOMO of the electrolyte is higher than the potential of the cathode [9]. The existence of such a layer was shown for LiMnO_4 , LiCoO_4 , LiNiO_2 , $\text{LiNi}_{0.8}\text{Co}_{0.2}\text{O}_2$ and LiFePO_4 by Edström *et al.* that coined the term "SPI" and showed it to always contain the same organic species, with the difference being the relative composition [78]. However, the thickness of the layer was rather dependent on the electrode material, as well as the inorganic species. The SPI does not exclusively form in organic electrolytes, but also in hybrid electrolytes. This has been shown for a LiFePO_4 cathode with an organic solvent/IL hybrid electrolyte. Furthermore, the interfacial resistance of the hybrid electrolyte was lower and resulted in a better cycling performance of the battery, when compared to the IL free conventional electrolyte [79].

3 From Li-salts to Polymerized Ionic Liquids (PILs)

In this chapter all the materials needed to create electrolytes for LIBs are discussed in terms of important properties as well as their specific advantages and disadvantages. Furthermore, their suitability as electrolyte materials for HT-LIBs are discussed.

3.1 Components

To create an electrolyte for a battery we need to combine several components - materials of varying complexity. Starting with the Li-salt, in its highest purity containing only a Li^+ and an anion, the addition of solvents increases the number of species present. Depending on both the types and number of solvents used, the overall complexity of the electrolyte can heavily differ, shown by the broadened base of the pyramid (Figure 6).

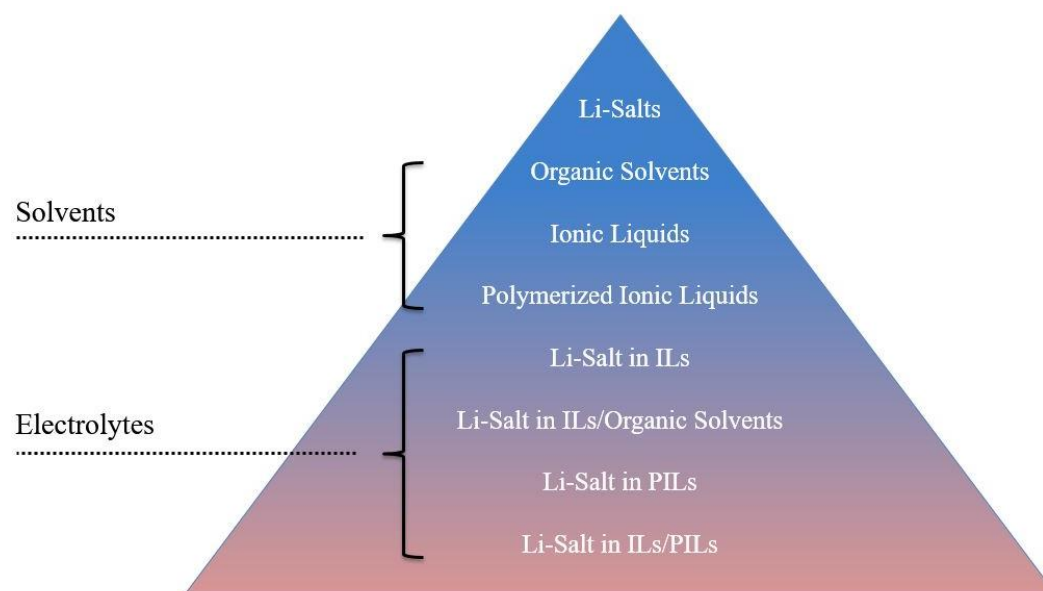


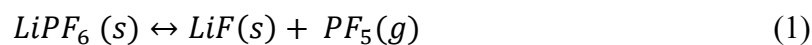
Figure 6: Increase in complexity from Li-salt to PIL based electrolytes.

3.1.1 Lithium Salts

The overall properties of the electrolyte are highly influenced by the lithium salt used. In general, it must be soluble enough in the matrix to enable concentrations of *ca.* 1 M in order to obtain optimal ionic conductivities [80]. Furthermore, it needs to produce stable SEI in interaction with the solvents [81], be non-corrosive towards electrodes and current collectors, as well as being non-toxic.

As mentioned above, LiPF_6 is the most common salt for electrolytes of LIBs [41], providing electrolytes with very high ionic conductivities at RT [82], wide ESWs, and stable SEIs [83]. The major drawback of this salt is its auto-decomposition reaction (1)

[84], which involves the release of gaseous PF_5 . At the same time, the production of solid LiF is often a wanted product for the SEI and F^- ions stabilize the Al current collectors by forming AlO_xF_y [85].



Another drawback is that the salt can react with trace water impurities to form highly toxic HF , in turn reacting with the SEI and positive electrode materials [86,87]. The decomposition of LiPF_6 , which becomes more severe with increasing temperature, restricts the upper operation temperature limit of LIBs to approximately 60°C [84]. Already at 55°C LiPF_6 and organic solvent based electrolytes start to show decreased cycle stability, however, this can be partly mitigated by adding lithium bis(oxalato)borate (LiBOB), which results in a more robust SEI [88].

The LiTFSI salt has been proposed as an alternative to LiPF_6 , in order to increase the thermal stability and improve the stability against water impurities [80,89]. LiTFSI based electrolytes have ionic conductivities comparable to those which are LiPF_6 based [80] and demonstrate stable operation at 60°C [90]. Improved discharge capacities have also been demonstrated across a wide temperature interval: -10 to 80°C [91]. A drawback, however is corrosion of the aluminium current collector above 3.6 V [92–94], by an anodic dissolution process of unprotected Al. This can be mitigated by adding a small amount of either LiPF_6 [91], LiBOB [95], or by using very high concentrations of LiTFSI , which form a protective film composed of LiF on the Al surface [96]. Furthermore, solvents containing a cyano-group can increase the stability against aluminium corrosion by up to 0.4 V by the cyano-group undergoing chemical reactions with Al intermediates, which compete with the electrochemical oxidation to Al^{3+} [97]. In an $\text{LiTFSI IL}_{\text{el}}$ aluminium corrosion has been prevented, possibly resulting from a protective layer containing Al^{3+} and TFSI [98,99].

The LiFSI salt is another alternative being increasingly studied, much due to its high thermal stability and the high ionic conductivity of its electrolytes [100–102]. LiFSI was reported to be stable up to 200°C and its electrolytes to exhibit higher ionic conductivities than those with LiPF_6 or LiTFSI [103]. The SEI formed is reported to be comparably smooth and uniform with respect to LiPF_6 based electrolytes [104,105]. However, there are contradictory reports about the thermal stability of LiFSI ; with a possible decomposition at 75°C [106] the suitability for HT-LIBs is unclear. A more detailed discussion of the fundamental as well as practical stability of the LiFSI salts available is presented in **paper I**.

LiBOB is another promising salt for HT-LIBs as it has a thermal stability of 300°C [107], as well as excellent oxidation resistance up to $4.6\text{ V vs. Li}^+/\text{Li}^\circ$ [108]. LiBOB also forms a very stable SEI on graphite anodes [109]. The ionic conductivity is usually lower [110], but have been reported on par with LiPF_6 based electrolytes [108]. LiBOB has a reported ability to suppress aluminium corrosion up to $5.5\text{ V vs. Li}^+/\text{Li}^\circ$ [111], as

well as enabling high-temperature cycling when added to a LiTFSI in an EC and ethyl methyl carbonate (EMC) based electrolyte [95]. Some drawbacks include moisture sensitivity, possibly producing boric acid [110], in addition to a limited solubility in organic solvents [112].

Lithium 4,5-dicyano-1,2,3-triazolate (LiDCTA) is a lithium salt free of oxygen and fluoro atoms, improving safety and lowering costs by an easier manufacturing process [113]. It is thermally stable up to 300°C making it interesting for HT-LIBs. However, its electrolytes have only modest ionic conductivities of 2.9 mS/cm [114] and a low anodic stability of *ca.* 4 V vs. Li⁺/Li^o [113,115].

The above results all arise from using solvents optimized for conventional lithium salts. In **paper VI** we characterize novel electrolytes based on LiDCTA in nitrile based solvents for physico-chemical properties [116]. Hundreds of lithium salts have been tested over the past decades for application in LIBs, but only less than ten have finally been established [117]. Even though the many drawbacks of LiPF₆, no other salt has succeeded in replacing it. For HT-LIBs no Li-salt at all has been established – yet. Possible strategies to enable HT-LIBs and to increase the thermal stability of the electrolyte without compromising other properties could be the combination of different salts/different solvents as well as to find the optimal concentration of each.

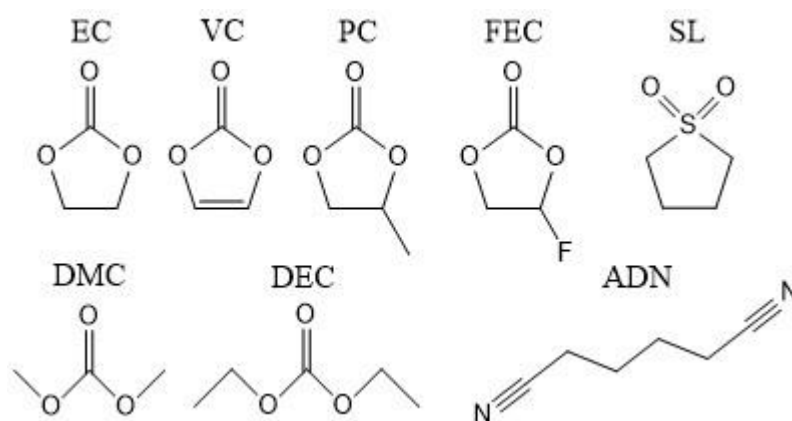
3.1.2 Organic Solvents

A solvent is needed to dissolve a substance (solute) and depending on the solute and solvent combination, the dissolution process can be more or less efficient. As a general rule of thumb, polar organic, *i.e.* carbon based, solvents are ideal to dissolve polar substances such as salts. The permittivity is used to classify the polarity of the solvent by its dielectric constant (ϵ) ($\epsilon > 15$: polar) [118] and a high dielectric constant favours the salt dissolution process [119]. Cyclic carbonates such as EC have relatively high dielectric constants, commonly > 60 and a low volatility at RT due to their high boiling points, generally $> 160^\circ\text{C}$, but their transport properties are rather limited due to their high viscosities > 2.5 mPa s (Table 5). Linear carbonates have lower dielectric constants of < 30 , but have generally low viscosities of < 1 mPa s and excellent transport properties. As a result, a combination of a cyclic and a linear carbonate provides the basic properties needed for a well-functioning electrolyte. Indeed, most LIB electrolytes contain a mixture of EC or VC with linear carbonates [71] (Figure 7). The main drawbacks of organic solvent mixtures, containing cyclic and linear carbonates, are their low flash points (FP) (*ca.* 30°C) and long self-extinguishing times (> 6 s/g), making them flammable mixtures [120,121]. In terms of HT-LIBs, another disadvantage is the high volatility of the linear organic solvents, increasing the pressure inside the cell and explosion in the worst case scenario. To overcome these performance and safety limitations, research has more recently focussed on alternative solvents such as fluorinated carbonates, sulfones, nitriles, ILs and PILs.

Table 5: Important properties of common organic LIB electrolyte solvents [119,120,122–130].

Organic Solvent	T _m [°C]	T _{b/d} [°C]	ε	η [mPa s]	FP [°C]	Flammable
EC	36.4	248	89.8	1.9 (40°C)	160	no
PC	-48.8	242	64.9	2.5	132	no
VC	20	162	127.0	-	73	no
DMC	4.6	91	3.1	0.6	18	yes
DEC	-43.0	127	2.8	0.8	31	yes
FEC	20	212	110	4.0	102	no
ADN	2	295	30	6.1	163	no
SL	28.5	287	43.3	10.3 (30°C)	151	no

Fluorinated organic solvent mixtures derived from DEC, ethyl acetate, ethyl methyl carbonate, *etc.* have been investigated by Achiha *et al.* and showed both higher anodic stabilities and higher thermal stabilities as compared to their non-fluorinated analogues [131]. Furthermore, good SEI forming capabilities such as low film and charge transfer resistances were achieved when di-2,2,2-trifluoroethyl carbonate, methyl-2,2,2-trifluoroethyl carbonate, *etc.* were part of the electrolyte, and they also showed good HT storage properties with only minimal capacity loss [132]. In **paper IV** FEC was investigated as part of an IL/organic solvent hybrid electrolyte (sub-chapter 3.2.2).

**Figure 7:** Structures of common cyclic and linear organic solvents.

Nitrile based solvents (as well as sulfones) have high oxidation stabilities and can be used as solvents for electrolytes with high voltage cathodes [125,133]. Adiponitrile (ADN) and sulfolane (SL) have been investigated as solvents and co-solvents of mixtures for nitrile based salts in **paper VI**. The investigated electrolytes are not viable for HT-LIBs due to their mass loss during isothermal TGA at 80°C. However, both ADN and SL can as co-solvents of EC increase the safety properties of the electrolyte by increasing the flash points and decreasing the heat generated upon cell failure [126,127]. The electrolytes tested in **paper VI** supported only moderate discharge capacities of 140 mAh/g for Li||LFP half-cells at 0.1 C and RT due to the high viscosities of > 14 mPa s.

3.1.3 Ionic Liquids (ILs)

ILs are by definition salts which melt $\leq 100^\circ\text{C}$ [134]. The temperature limit is not connected to any fundamental property and is thus a rather arbitrary choice [135]. When the melting point is below room temperature, the term "room temperature ionic liquids" (RTIL) is sometimes used – but herein we use IL for simplicity. The first known IL (ethanolammonium nitrate) was discovered in 1888 by Gabriel and Weiner [136], while the first RTIL (ethylammonium nitrate) was discovered in 1914 by Walden [137]. The number of known ILs has increased dramatically ever since, and the total number of potential ILs is estimated to be approximately one trillion (10^{18}) [19,138]. The huge number of possible cation and anion combinations, and IL properties, have given ILs the denomination “designer solvents” [139,140]. Indeed, the application of ILs stretches from HT stable lubricants [141], over pharmaceutical ingredients [142], to energy applications [22,143], and biomass conversion [144].

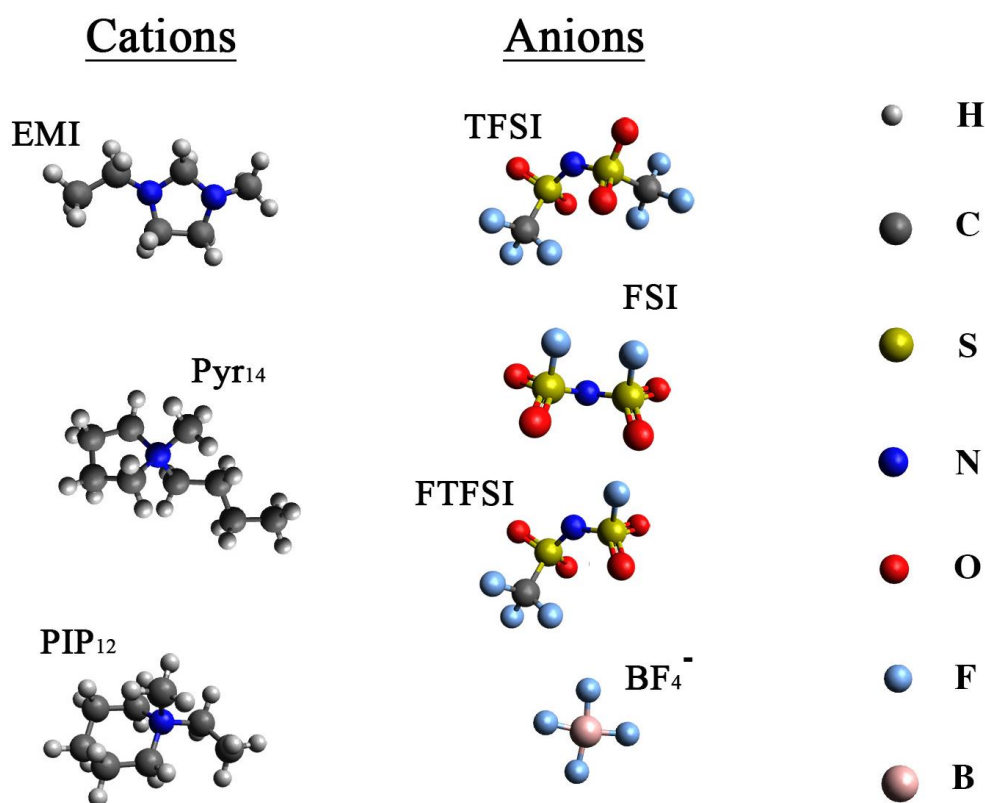


Figure 8: Structures of cations and anions of some ILs.

In general, ILs consist of large organic cations and inorganic anions both with a delocalized charge [21] (Figure 8). The exchange of a small monoatomic anion, *e.g.* Cl⁻ in the IL 1-ethyl-3-methyl-imidazolium chloride (EMICl), to the molecular and larger tetrafluoroborate anion (BF₄⁻), or the even larger bis(trifluoromethanesulfonyl)imide anion (TFSI) decreases the melting point of the corresponding ILs from 89°C to 11°C

to -15°C , respectively [145]. An exchange of the cation results in yet larger melting point differences [22], while altering the functional groups of the cation can induce a change of as much as 70°C [146].

The aforementioned effects of changes in IL cation/anion molecular structure have a large effect also on the thermal stabilities. Dynamic TGA assessment of Pyr_{1x} ($x = 3-10$) based ILs showed a decrease in T_d with increasing alkyl chain length, as well as a reduction of time to ignition (Table 6) [147], observed also for imidazolium and piperidinium based ILs [148,149]. Furthermore, some imidazolium based ILs (*e.g.* EMITFSI) have been classified as the “thermally most stable” ILs among 66 investigated ILs [148]. A strong influence of the thermal stability has the exchange of the counter-anion from TFSI to FSI, which leads to a reduction in T_d of *ca.* 100°C (Table 7) as reported in **paper II**. The structural change can, however, be more subtle: shorter alkyl chains of the cation can lead to decreased viscosities and increased ionic conductivities [150].

Table 6: Effect of the alkyl chain length on T_d and time to ignition [147].

Ionic Liquid	T_d [$^{\circ}\text{C}$]	Time to ignition [s]
$\text{Pyr}_{13}\text{TFSI}$	387	350
$\text{Pyr}_{14}\text{TFSI}$	383	325
$\text{Pyr}_{16}\text{TFSI}$	380	288
$\text{Pyr}_{18}\text{TFSI}$	360	278
$\text{Pyr}_{110}\text{TFSI}$	342	260

Many ILs have a long time to ignition and are therefore almost non-flammable and this, combined with very high FPs, makes them more suitable as electrolyte solvents for HT-LIBs as compared to organic solvents (Table 7 vs. Table 5). However, their high viscosities are a major drawback as it impedes (ion) transport.

Table 7: Properties of common ILs [122,133,151–157], [**II**,**III**].

Ionic Liquid	T_m [$^{\circ}\text{C}$]	$T_{b/d}$ [$^{\circ}\text{C}$]	η [mPa s]	FP [$^{\circ}\text{C}$]	Flammable
EMIFSI	-16	201	22	> 300	no
EMITFSI	-18	302	40	> 300	no
$\text{Pyr}_{14}\text{TFSI}$	-7	383	100	n/a	no
$\text{Pip}_{14}\text{TFSI}$	-10	334	256	n/a	no

3.1.4 Polymerized Ionic Liquids

PILs basically consist of the same cations and/or anions as in ILs. Either the cation, the anion, or both are, however, interconnected resulting in a polymeric backbone. The first PIL-imidazolium based homopolymer was created in 1973 [158]. However, the first time the term PIL was used was decades later, in 1998, for imidazolium and

sulfonamide PILs [159]. These had very high ionic conductivities compared to conventional polymers, in the range of 10^{-4} to 10^{-7} S/cm, while certainly not high compared to ILs or organic solvent based systems. The main advantages of PILs in comparison to ILs are mechanical stability and processability. Their similarity to ILs allow them similar fields of application, such as catalysis, CO₂ capture, electrochemical devices, *etc.* [160].

PILs are obtained from a polymerization of the IL monomer anion or cation creating covalent bonds from polymerizable groups such as vinyl, vinyl ether, (meth)acryloyl, *etc.* [24,161,162]. When only the anion or the cation is polymerizable, the covalently created polymer backbone can only consist of IL cations (polycation) or anions (polyanion), respectively. The mobility of the ions in the backbone is strongly reduced, thus the resulting PILs can be used to create single-ion conductors [163].

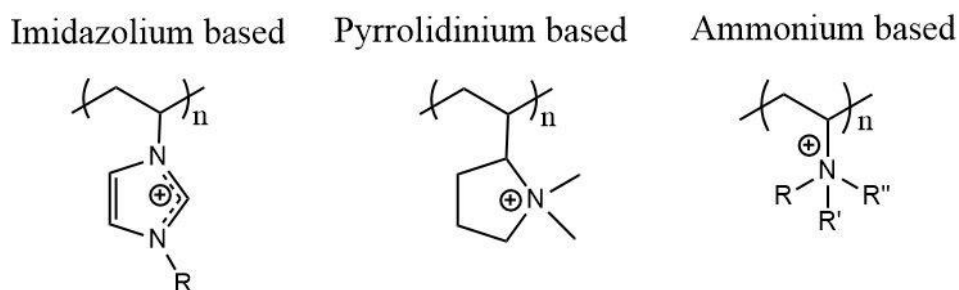


Figure 9: Cationic IL monomers for PILs.

Typical cationic PILs contain the imidazolium or pyrrolidinium cations (Figure 9) while many other polycationic PILs are possible. PILs are “designable”, just like ILs, by combining different cations and anions, changing the alkyl chain lengths, introducing a spacer, *etc.* [24,164]. Analogous to the ILs, the exchange of the anion in PILs can induce drastic changes in the properties; *e.g.* the change from PF₆⁻ to TFSI⁻ in an imidazolium based PIL was shown to increase the ionic conductivity by two orders of magnitude [165].

The ionic conduction mechanism in PILs is dependent on the number of repeating units, or analogously, the molecular weight (M_w) of the PIL. Fan *et al.* showed ammonium based PILs with ≥ 10 repeating units, to have a strong decoupling of the ionic conductivity/ion transport from the macroscopic viscosity and segmental relaxation [166]. The decoupling arises from increased M_w , which restricts the movement of the tethered cation and lowers its transference number close to zero. Additionally, the increased M_w imposes space restriction for the polymer chains. This decoupling of ionic conduction from the structural dynamics was also seen for xVITFSI based PIL resulting in a “super-ionic” behaviour [167] (Figure 10). Three possible transport/hopping mechanism for anions in polycationic BVI-PF₆ PIL were suggested: intramolecular hopping along the PIL backbone, intermolecular hopping between two different chains, and anion hopping from the PIL backbone to “free”. Molecular

dynamics simulations have shown that intramolecular hopping along the PIL backbone is the dominant mechanism, where a PF_6^- anion is associated to four monomers belonging to two different polymer chains. Upon increasing temperature, “free” anions become more likely [168]. The thermal stabilities of PILs is in general high, however, dependent on the ions contained. Nakajima *et al.* reported thermal stabilities of *ca.* 400°C for imidazolium based PILs, while Zhang *et al.* reported thermal stabilities of > 250°C for ammonium based PILs [169,170].

3.2 Electrolytes

3.2.1 IL Based Electrolytes

One of the many reasons why ILs have been considered for LIB electrolytes is their high intrinsic ionic conductivities. Ionic conductivities exceeding 0.1 mS/cm at RT are often requested for LIBs [171], and typically ILs have conductivities between 0.1 and 20 mS/cm at RT [172]. However, neat ILs are not sufficient as electrolytes; a lithium salt is necessary to ensure Li^+ transport between the electrodes. The addition of a lithium salt to an IL matrix, however, increases the ion-ion association, as *e.g.* probed by *ab initio* calculations for an imidazolium IL_{el} and the decrease of interaction energies when comparing EMI-FSI to Li-FSI (-79 to -143 kcal/mol) as well as by the viscosity increase from 17 to 21 mPa s at 30°C [173]. Furthermore, association of ions can effectively form neutral ion-pairs that do not contribute to the ionic conductivity. The concept of ionicity, both for pure ILs as well as electrolytes, describes the contribution of ions participating in conduction processes with respect of the total amount of ions present [174]. In general, the dependence of molar conductivities, Λ , and viscosities, η , of ILs can be described by the fractional Walden rule (2), where the exponent α corrects for differences in the activation energy of the molar conductivity and the viscosity [175].

$$\Lambda \eta^\alpha = \text{const.} \quad (0 < \alpha \leq 1) \quad (2)$$

A Walden plot, $\log \Lambda$ vs. η^{-1} , can be used to qualitatively describe the ionicity in ILs and IL_{el} (Figure 10). The closer the ILs or electrolytes are to the reference (0.01 M $\text{KCl}_{(\text{aq})}$) the larger the ionicity. ILs and IL_{el} far below the reference line are classified as “poor ILs”, those in close proximity to the line as “good ILs”, and the very few found above the line are “super ILs” [176]. These “super ILs” have higher ionic conductivities than what their viscosities would suggest, usually containing small, low charged ions which “escape the full viscous drag of the surrounding medium” [176] as seen for some PILs (Figure 10). The ion-ion association is considerable in “poor IL_{el} ” as seen by an increase in viscosity by Li-salt addition such as for a piperidinium/guanidinium based ILs (110 mPa s) and its 0.5 M LiTFSI IL_{el} (190 mPa s) resulting in low ionic conductivities (1.5 vs. 0.7 mS/cm) and a discharge capacity of only 100 mAh/g at 0.1 C

for Li||LFP half-cells [177]. A low ionic conductivity (0.16 mS/cm) and high viscosity (40 mPa s) was seen for tetramethylguanidinium 4-fluorophenolate (TMG4FPhO) based ILs [178] (Figure 10).

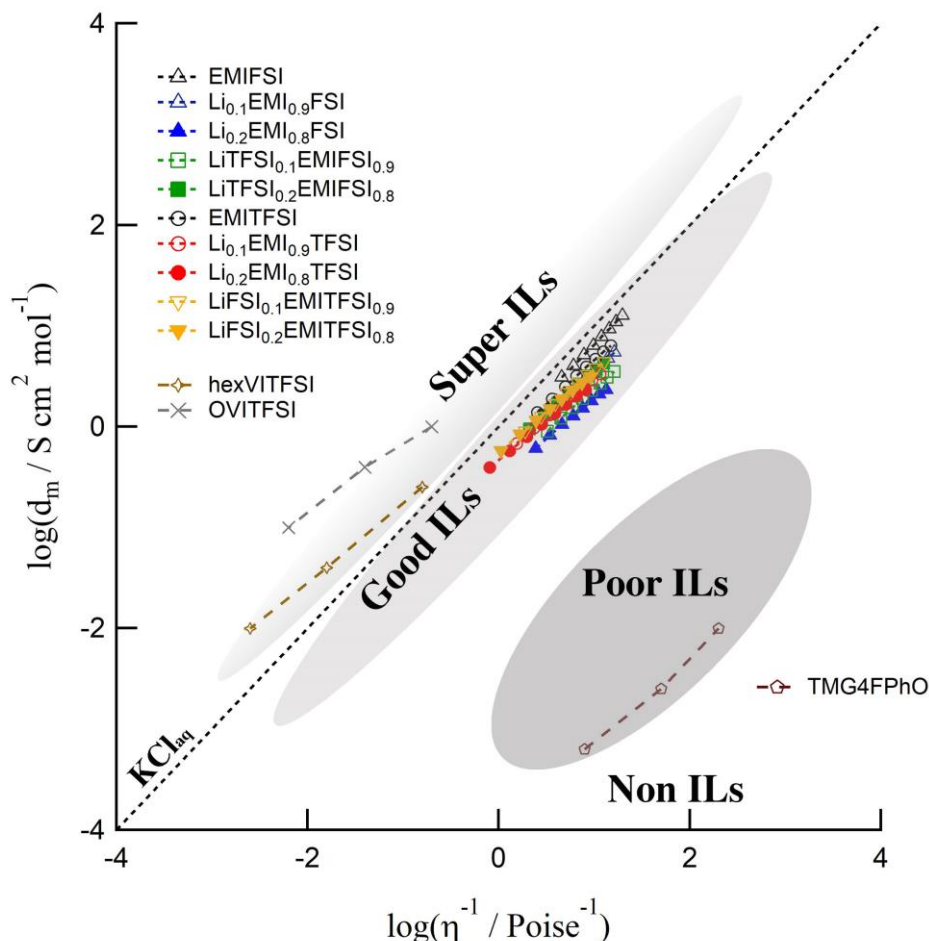


Figure 10: Walden plot with IL classification.

The Li^+ transference number, t_{Li^+} , the ratio of the Li^+ diffusion coefficient to the diffusion coefficient of all participating ions, should for a LIB electrolyte ideally approach unity [171]. The ion-ion association and the restricted Li^+ conductivity in “poor ILs” can lead to t_{Li^+} as low as 0.1 [179]. Furthermore, the proposed Li^+ transport mechanism occurs to be ineffective due to being vehicular by *ca.* 30%, Li^+ migrates together with its solvation shell (anions), and the remainder 70% by exchange mechanisms, similar to jumping or Grotthuss transport [180]. The implications are that bulky IL cations can have ten times as high mobilities as compared to the more associated Li^+ [181].

As mentioned for LIBs in general, a passivation layer or an SEI, often partly formed by the electrolyte, is needed to ensure good cycling stability [45]. For conventional organic solvent based electrolytes the reactions are complex between organic solvents, Li^+ and the graphite anode, but how is it for IL_{el} ? Yamagata *et al.* have proposed a double-layer

structure being formed on the surface of different carbon electrodes in EMIFSI and EMITFSI based electrolytes [182], while Xiong *et al.* argue for the existence of a SEI on lithium electrodes in a N-butyl-N-methyl pyrrolidinium (Pyr₁₄)TFSI based electrolyte [183]. An important question for HT-LIB application is thus SEI/double-layer stability at HT.

The most common ILs for battery electrolytes contain imidazolium (XMI) or pyrrolidinium (Pyr_{xy}) based cations [98,184] and the TFSI, FSI or BF₄⁻ anions [185–187]. Usually a lithium salt with the same anion as in the IL is added to the IL matrix [98,188], but a recent trend is to add a lithium salt with a different anion [67–70, **II**]. Novel anions have also been used *e.g.* the (fluorosulfonyl) (trifluoromethanesulfonyl) imide (FTFSI) (Figure 8), which in Pyr₁₄FTFSI exhibits no corrosion of Al current collectors up to 5 V *vs.* Li⁺/Li^o [193]. Furthermore, LiFTFSI based IL_{el} have wide ESW of 5.7 V [194] and showed a discharge capacity of 160 mAh/g of Li||LTO half-cells and an energy density of 131 Wh/kg for a LTO||LFP full-cell with coulombic efficiencies > 99%, both at 0.1 C [195].

Despite the aforementioned problems of ILs having high viscosities and low t_{Li^+} , IL_{el} show large promises, which in terms of capacity, rate capability and long-term cycle stability can lead to HT-LIB performance similar to or even surpass conventional LIB organic electrolytes [98,192]. In **paper III**, we showed a SnO₂ based electrode with a Pip₁₄TFSI IL_{el} at 80°C to perform as well as with an organic solvent based electrolyte at RT. Indeed, a phosphonium IL_{el} was tested in a Li||LiCoO₂ battery even at 100°C, but the electrochemical performance was, however, rather moderate [196].

3.2.2 Hybrid Electrolytes

IL/organic solvent hybrid electrolytes evolved from the idea to tackle the drawbacks of one solvent type by the advantages of the other, *e.g.* the high viscosity of ILs by use of organic solvents and the safety issues such as low FP and flammability of organic solvents by use of ILs. Altogether, a higher safety, increased reliability, and improved performance was foreseen to be achievable by this strategy [197].

For example, the physico-chemical investigations of the hybrid electrolyte 0.3 M LiTFSI in Pyr₁₄TFSI/PC showed a clear effect of the Pyr₁₄TFSI/PC ratio on the viscosities and ionic conductivities [122]. The electrolyte with 20 wt% PC and 80 wt% Pyr₁₄TFSI had a 70% lower viscosity than the pure IL_{el}, while at the same time the ionic conductivity increased from *ca.* 20 mS/cm to *ca.* 60 mS/cm. Guerfi *et al.* showed similar effects for electrolytes of 1 M LiPF₆ in different ratios of EMITFSI/EC:DEC:VC [198]. The viscosity increased with IL content, while the ionic conductivity had a maximum at 60% of IL. The maximum in conductivity can be understood by considering a preferred solvation of the Li⁺ cations by the organic solvents. Starting from 0% IL, the increase in IL content increases the amount of charge

carriers and up to 60% of IL, the Li^+ is still solvated by organic solvent molecules. For electrolytes with higher IL contents the amount of organic solvent molecules is not sufficient to solvate all Li^+ , which then start to be solvated by TFSI. The solvation of Li^+ by TFSI reduces the amount of charge carriers and the ionic conductivity decreases. Preferred coordination was also seen for Li^+ by EC and DMC in $\text{Pyr}_{14}\text{TFSI/EC:DMC}$ based electrolytes, which lead to enhanced low temperature conductivities [199]. Not only EC, but also other organic solvents such as tetrahydrofuran (THF) [200] can be preferentially coordinated by Li^+ as compared to ILs.

The influence on the transport properties is not the only effect; there is a drawback in terms of thermal stability and safety properties upon adding organic solvents. However, if the concentration of organic solvent is limited to *ca.* 20 wt%, also the hybrid electrolytes stay non-flammable, *e.g.* 20 wt% of PC in a $\text{Pyr}_{14}\text{TFSI}$ based electrolyte results in a non-flammable electrolyte, while ≥ 40 wt% results in flammable electrolytes [122]. This effect arises, again, from a preferential coordination of Li^+ by organic solvent molecules, which do not contribute to the flammability of the electrolyte as long as they are coordinated to Li^+ . However, when the number of organic solvent molecules exceeds the Li^+ coordination number, the amount of “free” organic solvent molecules increases and induce the flammability to the electrolyte. Furthermore, the salt concentration is important: LiPF_6 based electrolytes with 60 wt% of EMITFSI and 40 wt% EC:DEC turned non-flammable when ≥ 1 M LiPF_6 was used [201]. For lower Li-salt concentrations there are always “free” organic solvent molecules in the electrolyte, while by increasing the amount of Li^+ by adding Li-salt all the “free” organic solvent molecules eventually become coordinated and the electrolyte becomes non-flammable.

Hybrid electrolytes, such as the previously mentioned 0.3 M LiTFSI in different ratios of $\text{Pyr}_{14}\text{TFSI/PC}$ were cycled at 5 C and 60°C in Li||LFP half-cells. All the electrolytes showed similar 1st discharge capacities of *ca.* 130 mAh/g, but a high capacity retention (91%) after 500 cycles was only obtained for the electrolyte with high IL content (80% IL) [122]. In **paper IV**, we investigated pure $\text{Pyr}_{13}\text{TFSI}$ based as well as hybrid electrolytes with a low concentration (5-7 wt%) of different organic solvents added for HT-LIBs operating at 80°C. The performance of the Li||LFP half-cells improved for the hybrid electrolytes, especially at high C-rates. At 4 C-rate, a low concentration of FEC (6.6 wt%) improved the discharge capacities from 120 mAh/g to *ca.* 150 mAh/g and 300 stable cycles with high coulombic efficiencies (%) were performed. If we want to compare our $\text{Pyr}_{13}\text{TFSI/PC}$ based electrolyte to the above mentioned $\text{Pyr}_{14}\text{TFSI/PC}$ based electrolyte to elucidate any effects of the different alkyl chain lengths on the physico-chemical and electrochemical properties, the wt% differences for PC/IL and the LiTFSI concentrations (0.3 vs. 0.9 M) are unfortunately too large. Nonetheless, the impact of the constituent-concentrations as well as the temperature (60 vs. 80°C) on the electrochemical performance is seen by comparing discharge capacities of Li||LFP half-cells at 3 C for the two systems: 145 mAh/g vs. 160 mAh/g, respectively [122,202].

3.2.3 PIL Based Electrolytes

PIL based electrolytes (PIL_{el}) unite the advantages of IL and polymer based electrolytes: They can be thermally and mechanically stable and safer than organic based electrolytes [162]. Their ionic conductivities can be high; for both Li-salt/PIL electrolytes: 10^{-3} mS/cm [25], but especially for Li-salt/IL/PIL ternary electrolytes: 10^{-2} mS/cm [203].

Starting from IL monomers such as N-vinyl-3-ethyl-imidazolium TFSI (EVITFSI), the high ionic conductivity of the “monomeric” IL, 1 mS/cm at RT, is significantly lowered, 10^{-3} mS/cm at RT, when the cations or anions are polymerized to create the PIL [204]. In contrast to ILs, the ionic conductivity of a PIL increases when a Li-salt is added, 10^{-2} mS/cm, due to an increase in charge carriers [203]. This effect, however, is sustained only for a limited amount of lithium salt, *e.g.* as addition of 50 mol% of LiTFSI to imidazolium and piperidinium based PILs resulted in decreased ionic conductivities from $1.4 \cdot 10^{-1}$ to $2.8 \cdot 10^{-2}$ mS/cm and from $6.2 \cdot 10^{-3}$ to $2.6 \cdot 10^{-3}$ mS/cm, respectively [164]. Another possibility to increase the ionic conductivity is to tether the polymerized ion by a hydrocarbon chain such as the imidazolium cation of polymerized EVITFSI tethered by a dodecamethylene (-CH₂)₁₂ chain, resulting in 10^{-4} to 10^{-1} mS/cm, however, the addition of lithium salt thereafter only slightly increased the ionic conductivities [204].

The importance of the Li⁺ coordination and transport mechanism for IL_{el} has been discussed in sub-chapter 3.2.1, but how does the Li⁺ transport work in PIL_{el}? Very recently, studies on xVITFSI based PIL_{el} have shown that Li⁺ transport results from a combined mechanism by segmental motion of the polymer backbone, the charge carrier density, as well as the nanostructure of the PIL_{el} *e.g.* the backbone-backbone correlation distance [167]. Another study argues the local Li⁺ dynamics in LiTFSI/poly(diallyldimethylammonium) (PDDA) TFSI/Py₁₄TFSI ternary electrolytes at 50°C to be governed by only one mode of motion, where the Li⁺ is interacting with its solvation shell of TFSI anions [205]. The Li⁺ diffusion decreases from $1.2 \cdot 10^{-11}$ m²/s to $2 \cdot 10^{-12}$ m²/s when the PIL polymer content increases from 5 to 45 mol%, due to the increased viscosity with increased polymer content. At the same time, the activation energies for the local Li⁺ motion decreased from 20 to 15 kJ/mol by a beneficial effect of the cationic polymer interacting with the coordination shell of Li⁺, however, the motion of the ions on the long range scale is immobilised with increased polymer content.

The thermal stabilities of ternary PIL_{el} have been shown to be in the same range as their constituents [206]. Appetecchi *et al.* studied the LiTFSI/Py₁₄TFSI/PDDATFSI system and its constituents and found them to be stable up to *ca.* 350°C [206], but the neat PIL have by others [25] been reported to be stable up to 400-500°C, thus a decreased thermal stability when Li-salt is present. The structural dependency of both ILs and

PILs on the thermal stability is also true for PIL_{el}. In **paper V** we find the exchange of TFSI for FSI for the IL and PIL in LiTFSI/Py₁₄TFSI/PDDATFSI to decrease the thermal stability by 100°C.

From a HT-LIB point of view, ternary LiTFSI/Py₁₄TFSI/PDDATFSI PIL_{el} have been cycled in Li||LFP half-cells at 40°C and different C-rates [206]. Only at very low C-rates of 0.05 C, however, reasonable discharge capacities (148 mAh/g) were achieved, while already at 0.5 C they drop to 51 mAh/g [206]. In **V** we investigated similar PIL_{el} and half-cells, but with different ratios of Li-salt/IL/PIL and we achieved *ca.* 140 mAh/g at 0.5 C for 100 cycles at 80°C. Very recently, LiTFSI/EMITFSI/PDDATFSI ternary PIL_{el} with high IL content (80%) were shown to have higher discharge capacities at different C-rates than the Li-salt/IL analogues [207]. The improved electrochemical performance of the PIL_{el} was due to the increased ESW (5.0 *vs.* 3.9 V), lower interfacial resistance (160 *vs.* 330 Ω) and the higher t_{Li^+} (0.4 *vs.* 0.3) as compared to the IL_{el}. At RT and a 0.5 C-rate the PIL_{el} showed a discharge capacity of 154 mAh/g, 27 mAh/g higher than for the IL_{el}.

The physico-chemical properties of the here presented pure, hybrid and polymerized ionic liquid based electrolytes are all very promising for HT-LIB application, due to high thermal stabilities, good to very good ionic conductivities, and the obtained discharge capacities. However, there is still room for improvement, especially in terms of electrochemical performance at higher C-rates.

4 Experimental Techniques

A detailed characterization of both the constituents themselves and the resulting electrolytes is of utmost importance to understand the origins of their properties. In the following the main applied techniques, their purposes here, and the underlying theories and methods of data analysis are introduced.

4.1 Thermal Analysis Methods

4.1.1 Differential Scanning Calorimetry

Differential scanning calorimetry (DSC) is a common thermal characterization technique for all kinds of condensed phase materials where a qualitative and/or quantitative determination of any possible phase transitions is crucial. In ILs and PILs and for battery electrolytes in general, crystallization and glass transitions can limit the temperature application range, both for storage and operation.

DSC measures the heat flow of a sample compared to the heat flow of a known reference and the difference is monitored [208]. Two kinds of DSC exist; "Heat Flux" and "Power Compensated" [208]. The former, used here, is described in a schematic illustration of the DSC measurement chamber (Figure 11). In brief, a furnace is heated or cooled with a constant rate exposing two crucibles, one with sample and one reference, to the same heat flow. The temperature difference between the crucibles is recorded. Upon an endothermic phase transition, *e.g.* melting, the sample absorbs energy, which is observed as a feature in the DSC trace (Figure 12).

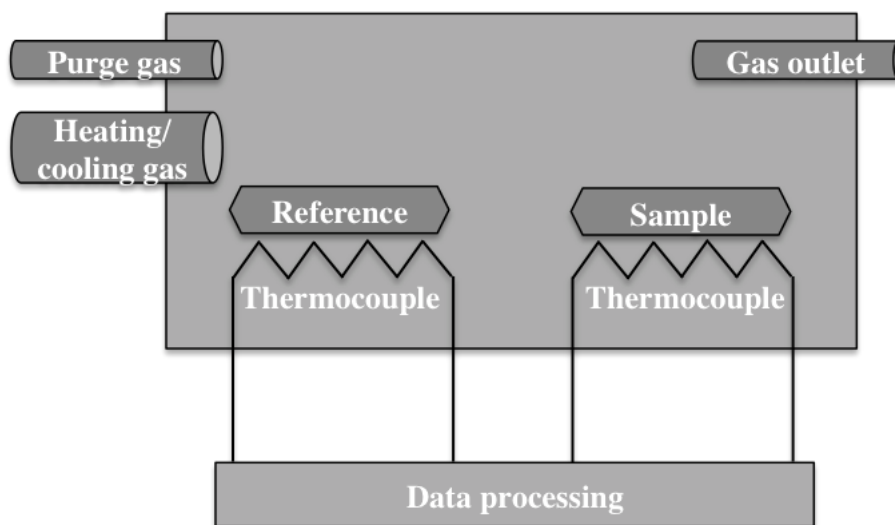


Figure 11: Schematic illustration of the DSC measurement chamber.

The DSC trace in Figure 12 is typical of an IL_{el}; flat until a glass transition (glass \Rightarrow liquid) occurs, for this particular electrolyte at *ca.* -86°C , ①, followed by an exothermal cold crystallization (liquid \Rightarrow solid) at -38°C , ②. Thereafter the solid directly melts, visible as an endothermic peak at -22°C , ③. To determine the features accurately, the on-set, the mid-point/inflection point, and the off-set temperatures, can all be used for the glass transition, while most often the peak maximum is used for defining crystallization and melting temperatures. In **paper I – III, V and VI**, we used (when present) the on-set temperature to determine the melting point and the inflection point to determine the glass transition, to accurately determine the T_g and the T_m .

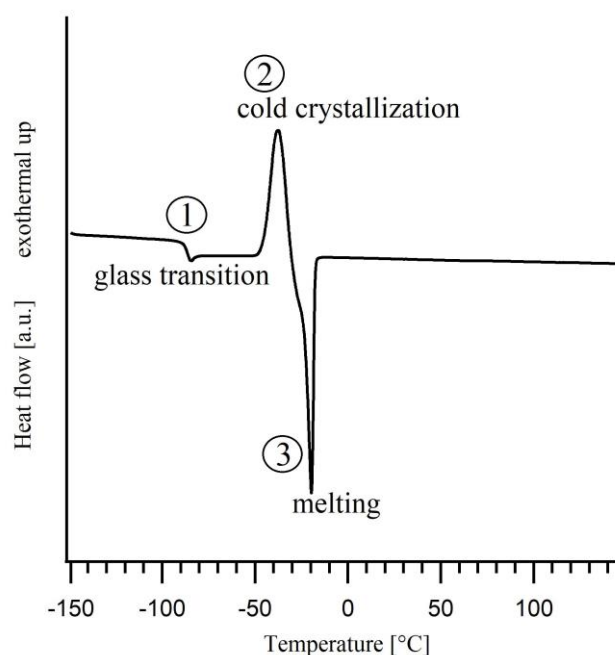


Figure 12: Typical DSC heating trace of an IL_{el}.

4.1.2 Thermogravimetric Analysis

In thermogravimetric analysis (TGA) a sample is heated while monitoring the mass change as a function of temperature and/or time. The main components of a TGA instrument are a heater, a temperature sensor, and a microbalance (Figure 13A). In general, TGA is performed to determine decomposition temperatures (T_d) or temperatures at which other mass loss processes, such as evaporation or sublimation, take place. Furthermore, decomposition without a change in sample mass is possible, and therefore undetectable *via* TGA, why other techniques, *e.g.* DSC, may provide complementary information. An inert purge gas (N_2 or Ar) is normally chosen to avoid oxidation and to not reduce the material's intrinsic decomposition temperature. The main functionality of the purge gas, however, is to remove reaction products, which otherwise may react further.

The choice of TGA crucible can also affect the results – usually aluminium crucibles are favoured, due to good thermal conductivity and low price. For temperatures above 600°C, however, crucibles of alumina or platinum are used.

The two most often used heating procedures are *dynamic* TGA, where the heating rate is constant, and *isothermal* TGA, where the sample is kept at a constant temperature for a certain time. T_d is mainly determined by dynamic TGA, while long-term stabilities and/or adsorption processes require isothermal TGA. Both methods were applied in **paper I - VI** for Li-salts, neat ILs, nitrile based solvents and electrolytes thereof, as well as for PIL_{el}.

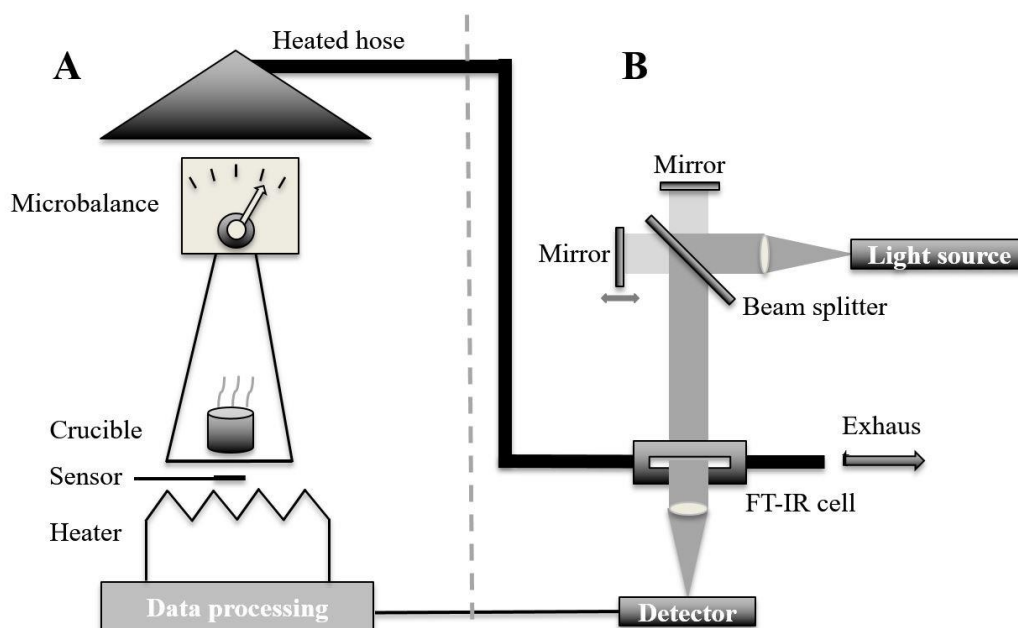


Figure 13: TGA coupled with FT-IR spectrometer.

A typical dynamic TGA heating trace displays the mass loss in % (Figure 14) as a function of temperature with process temperatures often defined by 1 or 5% mass loss ($T_{1\%}$ and $T_{5\%}$). An alternative is the extrapolated on-set temperature (T_{onset}) by using the intersection of the extrapolated baseline of 0% mass loss and the extrapolated tangent of the inflection point (Figure 14). T_{onset} is the temperature at which a reaction occurs spontaneously. The three temperatures are often used to determine the stabilities of samples, but to improve the reproducibility for samples without distinct decomposition processes it is recommended to use a reacted fraction (α), e.g. $\alpha = 0.05\%$ of the complete mass loss [209]. At the end of the heating curve, the off-set temperature (T_{offset}) – determined analogously to T_{onset} – can evaluate the completeness of a process (not shown). When the nature of the decomposition products is of importance, a set-up with a TGA coupled to a spectrometer, most often mass (MS) or Fourier-transform infrared (FT-IR), can provide additional information.

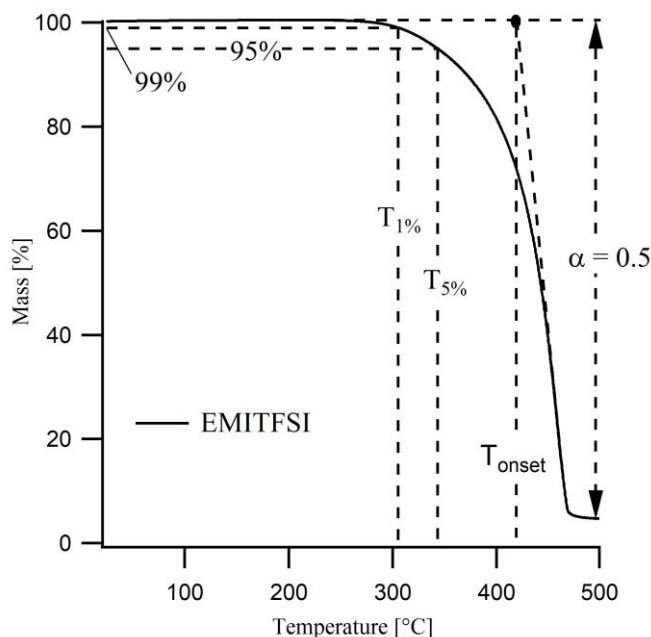


Figure 14: TGA data analysis by different methods.

The advantage of a TGA-FT-IR set-up is the possibility to identify decomposition products in real time and increase the understanding of the decomposition processes. The purge gas of the TGA carries the evolved decomposition products via a heated hose to the FT-IR spectrometer (Figure 13A and B), which continuously records spectra. A predefined number of these spectra are directly averaged to improve the signal to noise ratio of the resulting spectra – at the cost of decreased time-resolution. As the decomposition products are transferred from the TGA furnace to the FT-IR cell, there is also an inherent lag time (often minutes) – to be corrected for before correlating the FT-IR spectra features to the mass loss process(es). We made use of a TGA-FT-IR set-up in **paper I** and **VI** to elucidate (differences in) the gaseous decomposition products.

4.2 Dielectric Spectroscopy

Dielectric or impedance spectroscopy measures the frequency dependent impedance $Z^*(\omega)$ of a sample, which relates to its dielectric properties. These are determined by exposing the sample to an alternating electric field and measuring its current and phase response.

The presence of an electric field generates different polarization effects; free charges are displaced in and against the direction of the electric field (atomic or ionic polarization), while dipoles orient themselves with the positive and negative pole in respective direction (dipolar polarization). For alternating electric fields, the response of a material is dependent on the applied frequency: both effects are present at low frequencies, while the orientational polarization disappears as a result of inertia when the frequency is increased to approximately 10^{10} Hz. At 10^{13} Hz the alternating electric

field switches too fast for the atomic polarization to react, and finally at 10^{16} Hz not even the electronic polarization, where the electron cloud shifts with respect to the atomic core, is displaced anymore [210] (Figure 15). Thus, different effects can be targeted as a function of frequency; for IL_{el} the ionic conductivity is the property of interest where all ions participate: Li⁺, the IL cation, the IL anion, and the anion of the lithium salt. Furthermore, Li⁺ can be coordinated to the anions and migrate as part of different larger complexes and aggregates, why the main part of the conductivity does not necessarily arise from Li⁺ species [211].

A schematic of the cell used (Figure 16) shows: two electrodes placed in a brass casing, where Teflon[®] acts as an insulator and defines the volume of the sample. The physics behind this technique is that an oscillating potential difference between two electrodes (eq. 3), with ω as the angular frequency $\omega = 2\pi f$, leads to an alternating direction of the electric field. The resulting polarization effects can be measured as the alternating current response (eq. 4). The phase difference, ϕ between the applied voltage and the measured current is due to the time needed for polarization effects to get oriented.

$$U^*(t) = U_0 \exp(i\omega t) \quad (3)$$

$$I^*(t) = I_0 \exp(i\omega t + \phi) \quad (4)$$

The ratio between the complex parts of the applied voltage and measured current (eq. 5) gives the impedance $Z^*(\omega)$, from which the permittivity of the electrolyte, $\varepsilon(\omega)$, (eq. 6) and $\sigma(\omega)$ (eq. 7) are extracted. In this work, **paper II – VI**, frequencies between 10^{-1} and 10^7 Hz were routinely applied to extract the ionic conductivity.

$$Z^*(\omega) = \frac{U^*(\omega)}{I^*(\omega)} \quad (5)$$

$$\varepsilon(\omega) = \frac{1}{i\omega C_0 Z(\omega)} \quad ;(C_0, \text{ empty cell capacity}) \quad (6)$$

$$\sigma(\omega) = i\omega \varepsilon_0 \varepsilon(\omega) \quad ;(\varepsilon_0, \text{ vacuum permittivity}) \quad (7)$$

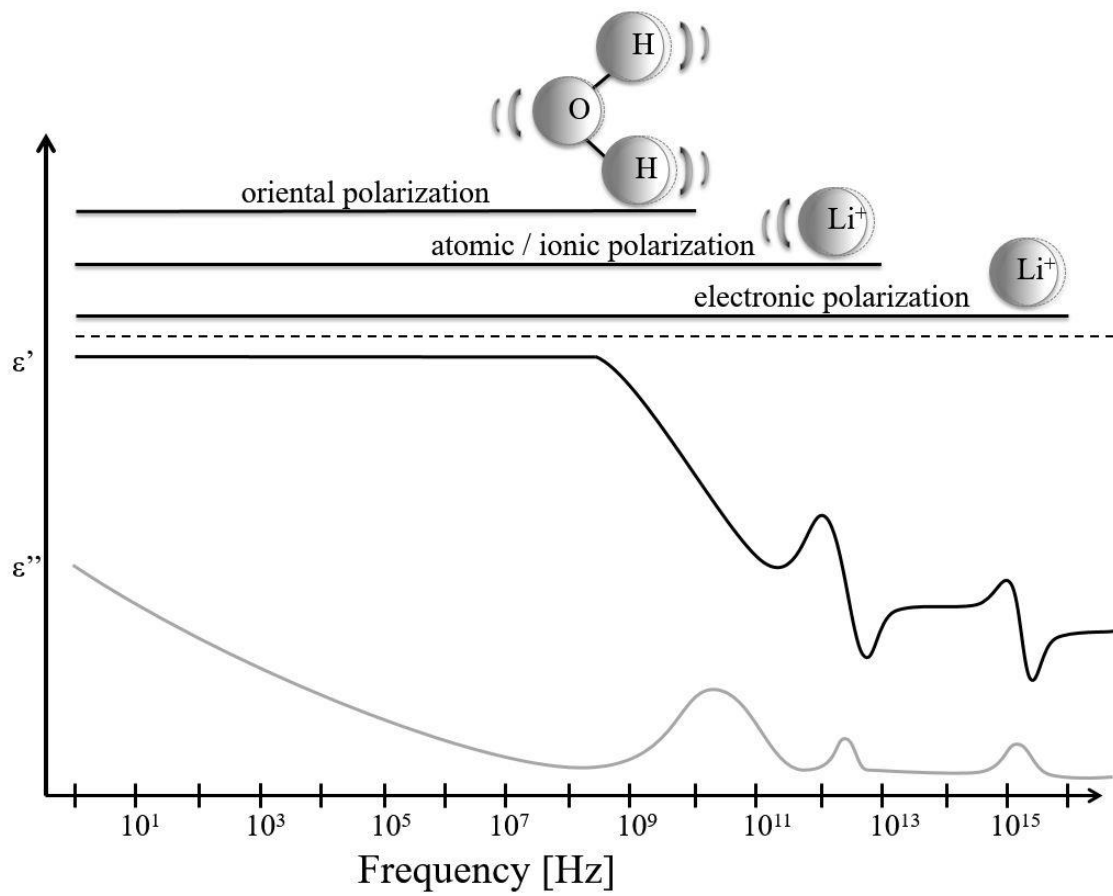


Figure 15: Physical origins of sample responses to electric field.

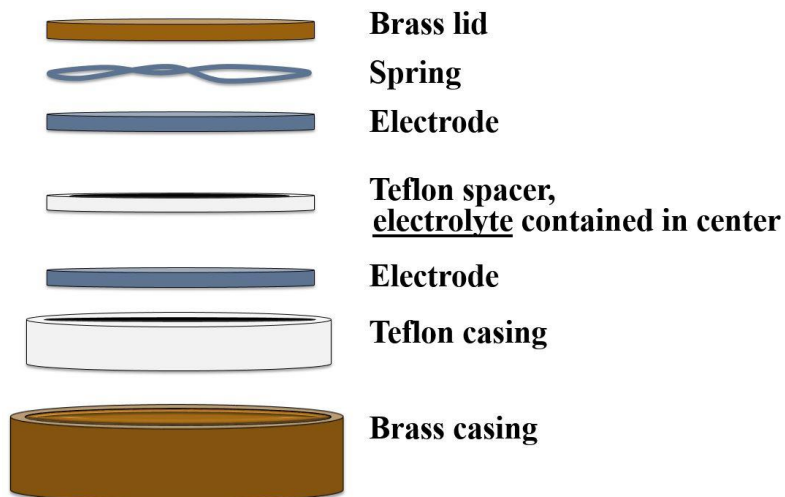


Figure 16: Dielectric spectroscopy measurement cell set-up.

4.3 Vibrational Spectroscopy

Vibrational spectroscopy comprises the interaction of electromagnetic waves with matter. Depending on the molecules, their symmetry and the atoms involved, only certain frequencies of electromagnetic waves induce vibrational modes. Every molecule consists of a certain number of atoms, which determine the degree of freedom of the molecule. In Cartesian coordinates, every atom (N) in the molecule can move in three directions ($3N$), but there are three combinations that describe the movement of the whole molecule (translations) and additionally three where it rotates as a whole (rotations), which leaves a total of $3N-6$ vibrational degrees of freedom. For a linear molecule two of the rotations are identical, which results in $3N-5$ vibrations. All vibrations contain changes of interatomic lengths and/or angles with characteristic frequencies. Even if a correct treatment demands quantum mechanics to be applied, a classic simple spring model can very well be used to visualize the factors determining the different frequencies [212]: an atom is bound to a large mass by a weightless spring with a characteristic force constant, f . A force F has to be applied to move the atom a distance x out of its equilibrium position x_0 . This force is in opposite direction to the force holding the atom in its position. The resulting equation is known as Hooke's law (eq. 8).

$$F = -fx \quad (8)$$

Newton's second law describes the relation of force, mass, and acceleration:

$$F = m \frac{d^2x}{dt^2} \quad (9)$$

Equating these two formulas gives:

$$m \frac{d^2x}{dt^2} = -fx \quad (10)$$

The following equation is the solution to (eq. 10) and describes a harmonic oscillator:

$$x = x_0 \cos(2\pi\nu t + \varphi) \quad (11)$$

Combining the equations above and solving for the frequency ν gives:

$$\nu = \frac{1}{2\pi} \sqrt{\frac{f}{m}} \quad (12)$$

Equation (12) determines the frequency with which a mass is vibrating when connected to a very large mass by an elastic spring. Thus the force constant (*i.e.* bond strength) and the mass (atom number incl. isotope) determine the vibration frequency – the stronger the atoms are attracted to each other and the lighter they are the higher the vibration frequency.

4.3.1 IR Spectroscopy

Infrared (IR) spectroscopy uses mid- and far-infrared light with wavelengths from 2.5 to 1000 μm to analyse matter [212]. A sample is exposed to a continuous infrared spectrum with the intensity I_0 . Depending on the bonds and atoms and the concentration, vibrational states are excited by photons (Figure 17). These photons are absorbed by the material and lead to absorption bands in the resulting spectrum. In an IR spectrum the transmittance, T , spectrum is provided (I/I_0) (eq. 13) as a function of wavenumber $\bar{\nu}$, where the wavenumber is the inverse wavelength.

$$T = \frac{I(\bar{\nu})}{I_0(\bar{\nu})} \quad (13)$$

The absorption, A , is proportional to the sample thickness or light path of the light beam, l , the molar absorptivity, ε , and the concentration of the absorbing species, c (eq. 14). This makes IR spectroscopy not only a qualitative, but also a quantitative tool. For a vibration to be IR active it must change the molecular dipole moment, μ , why diatomic molecules like O_2 and N_2 are not detectable by IR spectroscopy.

$$A = l \varepsilon c \quad (14)$$

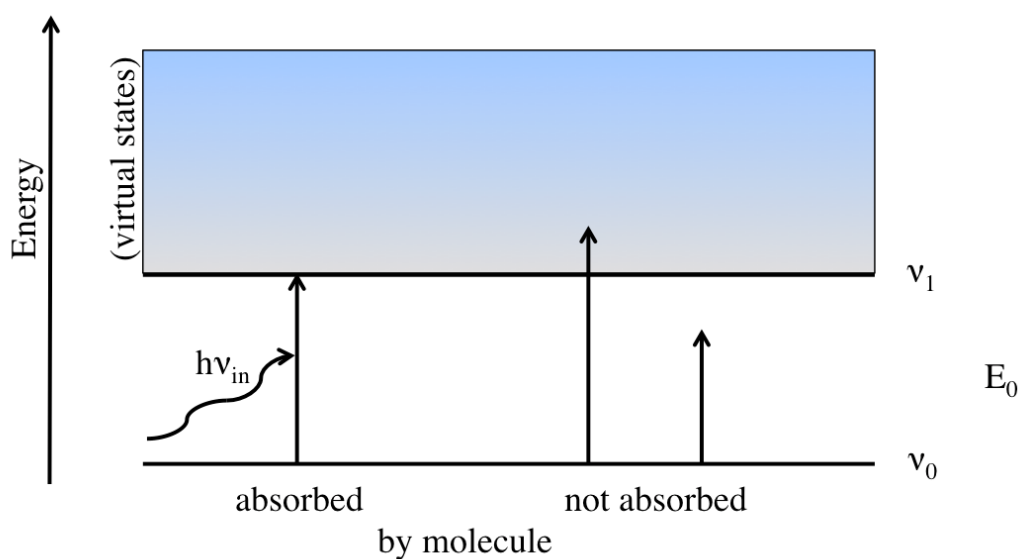


Figure 17: Absorption of photons by the transition of vibrational states.

4.3.2 Raman Spectroscopy

The Raman effect is due to the change of energy of a photon when a monochromatic laser beam irradiates matter [213]. A vibrational state is temporarily raised to a “virtual state”, energetically situated between the highest vibrational and the next highest electronic state. This transition is not quantized and the resulting emitted photon has either a lower energy (Stokes scattering), higher energy (anti-Stokes scattering) or the same energy (Rayleigh scattering) as the incident photon (Figure 18). At room temperature, the molecule is usually in its ground state and hence its vibrations (ν_0). Accordingly, the probability of detecting Stokes transitions are higher than anti-Stokes – resulting in higher intensities and a better signal to noise ratio why usually only the Stokes part of the Raman spectra is considered.

As for IR, Raman spectroscopy is qualitative and quantitative as the intensities of vibrations are proportional to the density of scattering molecules. An example of a section of a Raman spectrum together with its fitted bands and their vibrational origins are shown in Figure 19. The same molecule can give rise to a band at a shifted wavenumber when in a different local surrounding, as *e.g.* bond strengths can be changed.

For a vibration to be Raman active it must change the polarisability of the molecule, why homo diatomic molecules are Raman active and detectable (in contrast to IR). As a rule of thumb, symmetric molecules are Raman active, while asymmetric molecules are IR active, why Raman and IR spectroscopy (often) are considered as highly complementary methods.

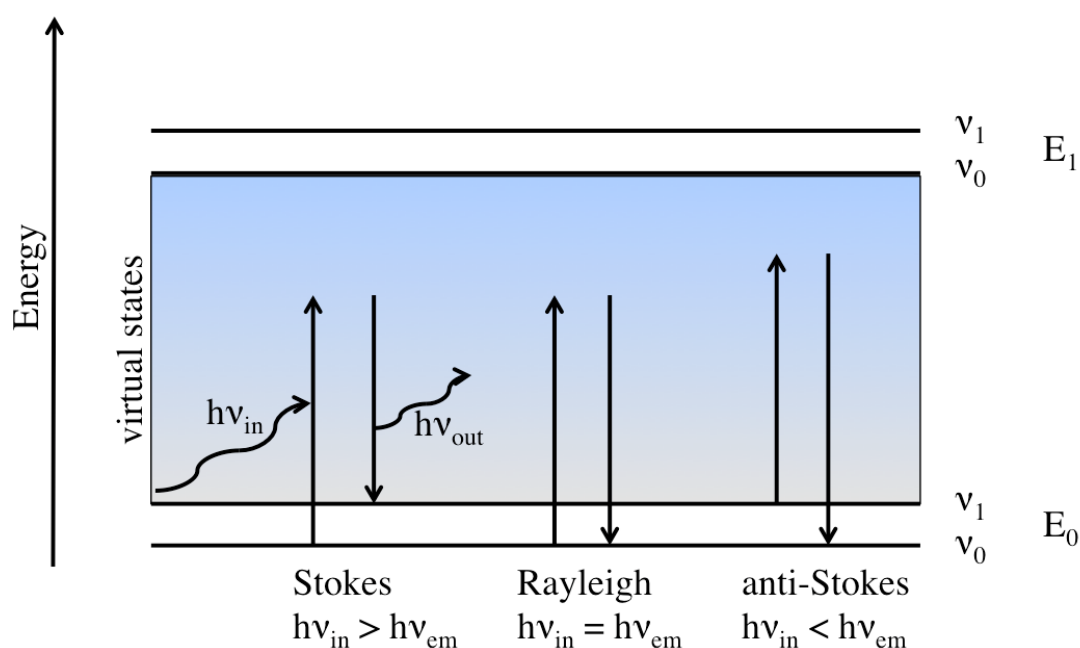


Figure 18: Vibrational transitions during spectroscopic measurements.

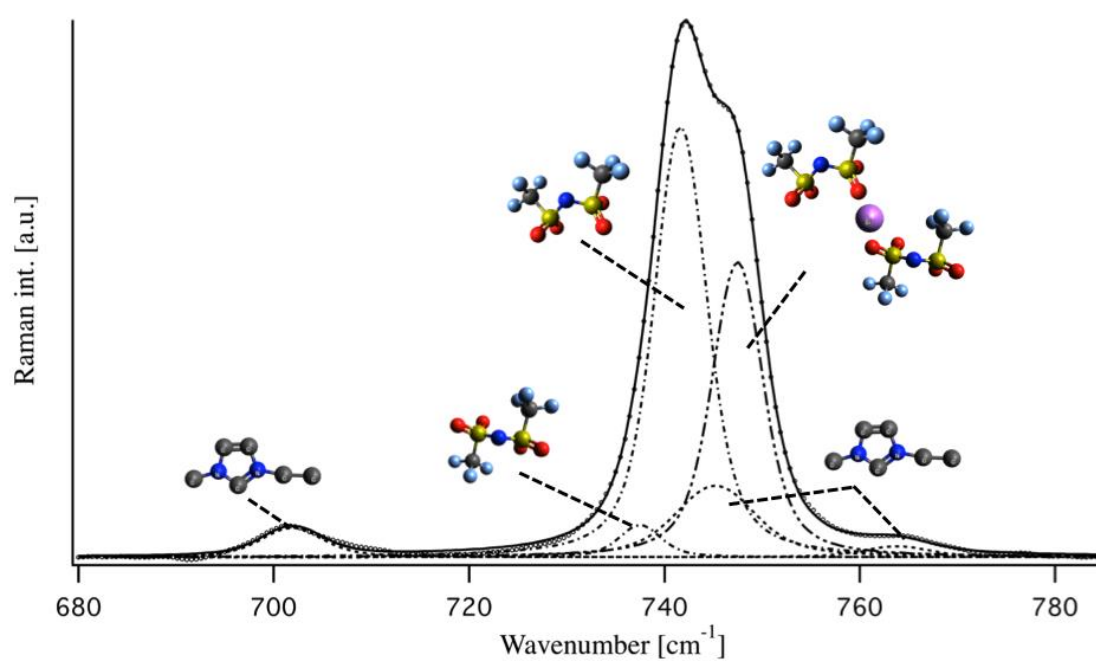


Figure 19: Raman spectrum of $\text{Li}_{0.2}\text{EMI}_{0.8}\text{TFSI}$ with band assignments.

4.4 Electrochemical Techniques

Electrochemical techniques are invaluable to test electrolytes for their viability in HT-LIBs and batteries in general. The width of the ESW and the quality of the SEI are common properties of/associated with the electrolyte, but also rate capability and capacity retention as a property of the electrode material can be limited by the electrolyte. All these properties can be investigated by electrochemical techniques.

4.4.1 Linear Sweep Voltammetry

Linear sweep voltammetry (LSV) is used to determine the ESW of the electrolyte [214] – an important property that gives a first hint of viable electrolyte-electrode combinations and working ranges [215]. Experimentally, a separator is soaked with electrolyte (for liquid electrolytes) and placed between two electrodes, usually in a “coin” or “Swagelok” type electrochemical cell (Figure 20A). For characterizing LIB electrolytes, lithium is most often used as reference (RE) and counter electrode (CE), while the working electrode (WE) is usually made of stainless steel, platinum, or gold [214]. Starting from the open circuit voltage (OCV), where no net current flows, the potential vs. $\text{Li}^+/\text{Li}^\circ$ is increased at a constant sweep rate, *e.g.* 0.5 mV/s. The measured current increases with the appearance of oxidative processes. Often, a cut-off current density of 0.1 mA/cm² is used to determine the starting point of electrolyte degradation. Separate runs using separate cells are made for the oxidative stability and the reductive stability. A typical LSV curve, a voltammogram, for one of the electrolytes from **paper II** is shown in Figure 20B, with an ESW of *ca.* 5 V.

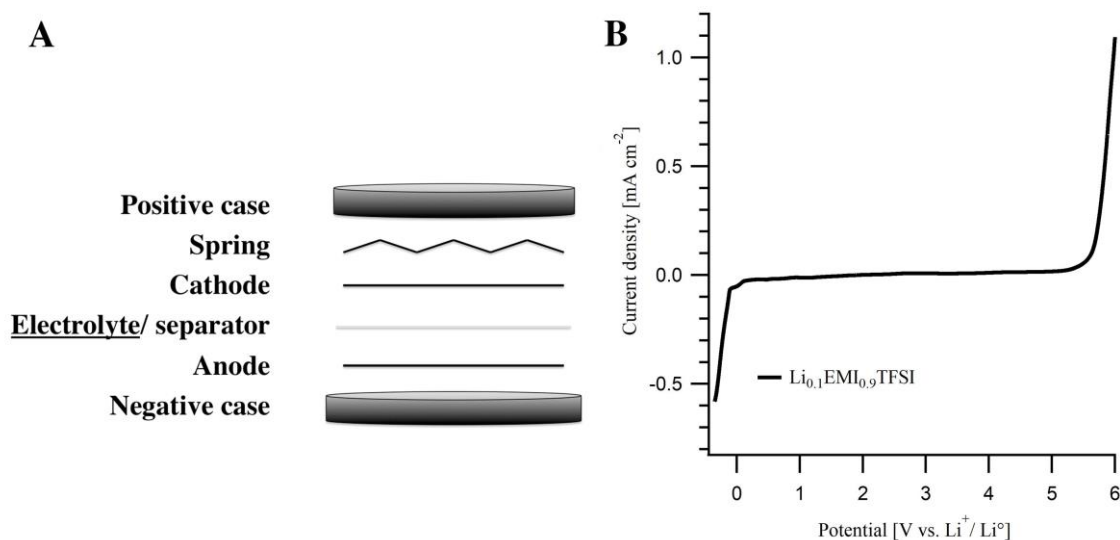


Figure 20: Electrochemical test cell and a typical voltammogram.

4.4.2 Impedance Spectroscopy

Electrochemical impedance spectroscopy (EIS) is a powerful tool to investigate electrode/electrolyte interfaces such as the evolution of the SEI. Similar to dielectric spectroscopy (sub-chapter 4.2), also here, a sinusoidal potential is applied (eq. 3) and a sinusoidal phase shifted current response (eq. 4) monitored. The complex impedance is received from the ratio of potential and current (eq. 5). Analysing the impedance data is far from trivial and often equivalent circuits of components such as resistors and capacitors are used to match the response from the system [216]. These components are to represent plausible physical processes of the system such as charge transfer, double layer formation, *etc.* Figure 21A shows the equivalent circuit for a Li|electrolyte|Li symmetrical cell used in **paper V** to determine the interfacial resistance between Li and PIL_{el}. A diagram typically used to characterize the impedance of the investigated system are called Nyquist or Argand plots [216] (Figure 21B). The negative imaginary part of the impedance is plotted *vs.* its real part. Every point in this plot is derived from one frequency. Figure 21B shows the Nyquist plot for one of the PIL_{el} investigated in **paper V** where frequencies in the range of 0.1 Hz to 200 kHz were applied.

The end of the semicircle at lower Z_{Re} (higher frequencies) determines the resistance of the electrolyte, while the end of the semicircle at higher Z_{Re} (lower frequencies) gives the sum of resistances of electrolyte and SEI [217]. Hence, the resistance of the SEI is the diameter of the semicircle. Most often no perfect semicircles are received, why programs such as Boukamp are used to extrapolate the semicircle and derive reliable resistances [218,219].

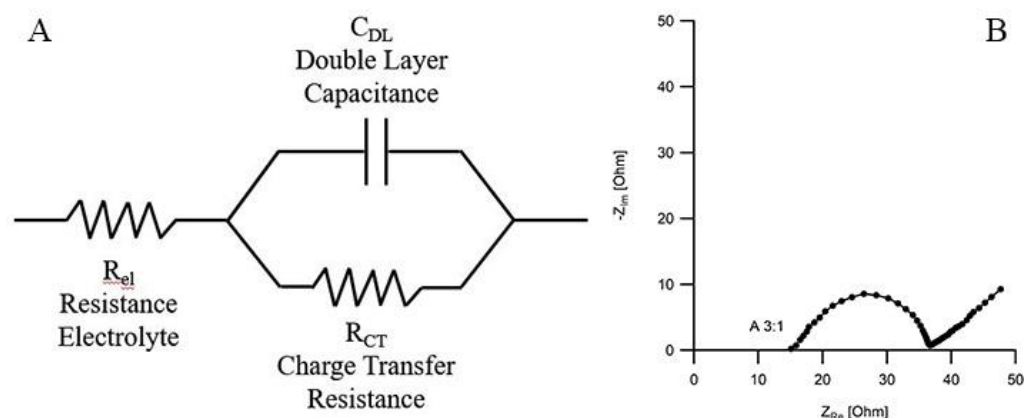


Figure 21: Equivalent circuit (A) and corresponding Nyquist plot of a PIL_{el} (B).

4.4.3 Chronopotentiometry

Chronopotentiometry is an electrochemical technique used to analyse electrode materials in battery cells and half-cells providing information on their rate capability, capacity retention, and viabilities for different electrolytes. The technique applies a controlled, most often constant, *galvanostatic*, current between the WE and CE and monitors the cell voltage between WE and RE [220]. In a two electrode setup, the same physical electrode functions as both RE and CE.

In cyclic chronopotentiometry the sign of the current (pos./neg.) is alternated to dis-/charge battery cells. Cut-off voltages set the dis-/charge limits, while currents determine the duration to dis-/charge a cell. Both settings depend on the electrode material, but can be limited by the transport properties and the electrochemical stability of the electrolyte. Often the applied constant current is expressed as a multiple of the theoretical specific capacity; the C-rate [29], where 1 C and 0.1 C is a current of 170 mA/g and 17 mA/g of active mass of LFP electrode material, respectively. In **paper V** and **VI**, C-rates between 0.1 C and 2 C were applied to characterize the rate capability of LFP electrodes using different PIL_{el} and nitrile based electrolytes (Figure 22).

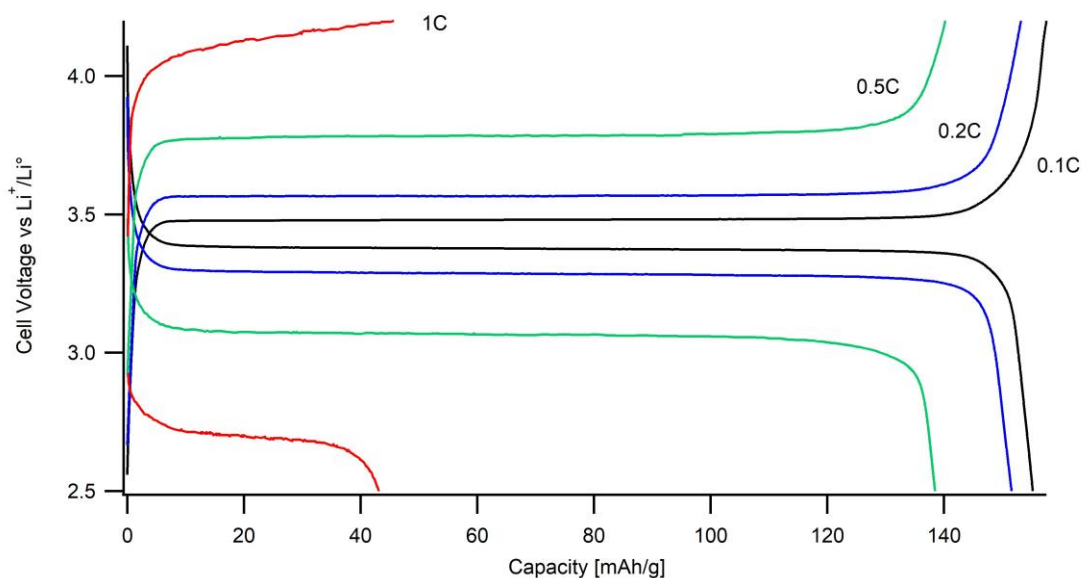


Figure 22: Rate capabilities of an LFP electrode using a PIL_{el} [V].

5 Summary of Appended Papers

5.1 Paper I

Thermal stability and decomposition of lithium bis(fluorosulfonyl)imide (LiFSI) salts

Three commercial LiFSI salts were compared in terms of their thermal stabilities and phase transitions to assure a high and uniform quality of this relatively new Li-salt. Additionally, we performed a combined Raman and IR vibrational spectroscopy analysis in order to find any molecular level differences, if possible. Indeed, Raman spectroscopy uncovered an impurity (LiClO_4) in one of the salts, likely a left-over from the synthesis process. This impurity was likely also the cause for the additional decomposition feature observed in the TGA data (Figure 23, trace B). However, the impurity did not affect the battery cycling with LFP electrodes during the first 50 cycles. While we did not observe any effect on the battery cycling performance, the thermal data illustrates a decreased stability due to the impurity and demands a more extended battery cycling to elucidate a possible effect on long-term cycling.

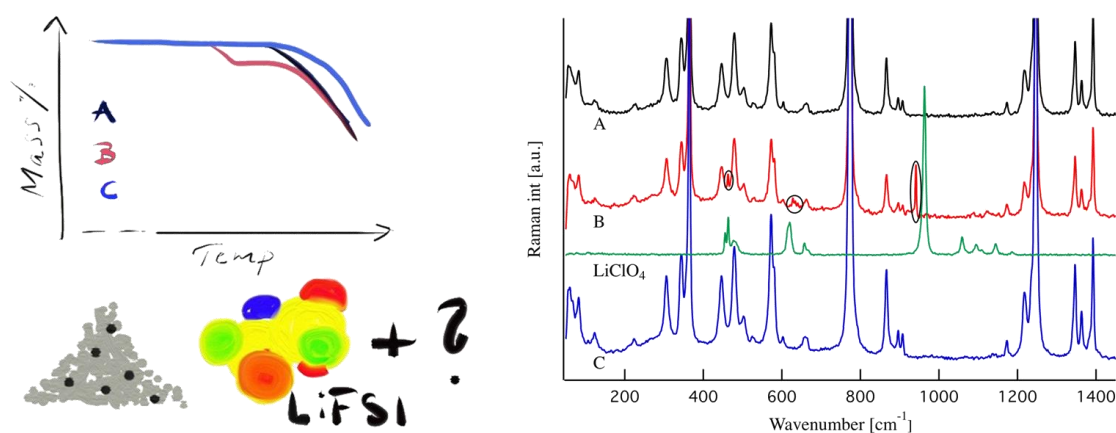


Figure 23: Dynamic TGA results and Raman spectra of three LiFSI salts.

5.2 Paper II

Ionic liquid based lithium battery electrolytes: Fundamental benefits of utilizing both TFSI and FSI anions?

The viability of IL_{el} for HT-LIB application with a special focus on a synergetic effect of having two anions present in the electrolyte were investigated by characterizing the fundamental properties of IL_{el} . All of the analysed electrolytes had wide liquid ranges and were thermally stable above $160^{\circ}C$ and even exhibited long-term stabilities over 10 hours at $100^{\circ}C$ (Figure 24). The ionic conductivities were acceptable at RT and further increased with temperature; showing excellent ionic conductivities at $90^{\circ}C$, together with the high-thermal stability suggesting their application in HT-LIBs. The $LiTFSI_{0.2}EMIFSI_{0.8}$ electrolyte where two anions are present was especially promising, outperforming the other electrolytes in terms of thermal stability and ionic conductivity. The ESW of the IL_{el} was ≥ 4 V and increased with TFSI content (Figure 24), enabling the IL_{el} to work with the most common electrode materials, while the IL_{el} with high TFSI content possibly work with high-voltage cathodes.

A detailed Raman analysis showed Li^{+} solvation numbers of *ca.* 2 for all the electrolytes, while the solvation numbers for the FSI based electrolyte were somewhat larger. No distinct anion coordination preference for Li^{+} was to be concluded, as the data were ambiguous. Possibly $LiTFSI_{0.2}EMIFSI_{0.8}$ indicates a synergetic effect of mixed anion IL_{el} demanding for research on other anion combinations in different cation based IL_{el} .

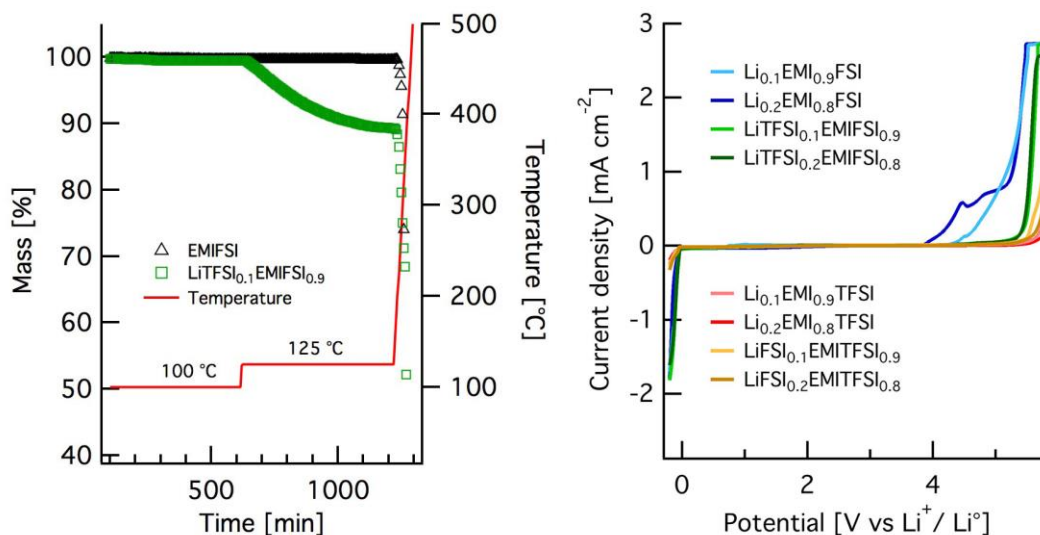


Figure 24: Thermal stability of an IL, an electrolyte, and ESWs of all electrolytes.

5.3 Paper III

Elevated temperature lithium-ion batteries containing SnO₂ electrodes and LiTFSI-Pip₁₄TFSI ionic liquid electrolyte

A 0.5 M LiTFSI in Pip₁₄TFSI IL_{el} was studied in terms of physical properties and electrochemical performance with a SnO₂ based electrode for suitability for HT-LIBs with increased energy densities. The electrolyte had a wide liquid range with a T_g of -68°C and a thermal stability of 339°C. Its “long-term” thermal stability was approved at 125°C where it was kept for 10 hours and showed no mass loss (Figure 25), enabling its storage and usage at HT. The electrolyte had a relatively low ionic conductivity at RT and just surpassed 1 mS/cm at 40°C (Figure 25), however, it further increased with temperature making it not only stable at HT, but suggesting its preferential application temperature in LIBs to be at HT. The cycle performance of SnO₂ based electrodes with the IL_{el} at 80°C was on par with the commercial LP40 electrolyte at RT. For the first 15 to 20 cycles, however, the IL_{el} showed larger irreversible capacity losses which could be connected to the reduction of the IL_{el}, leading to an increased thickness of the SEI of ≥ 10 nm, leaving room for improved SEI by *e.g.* addition of other salts or solvents.

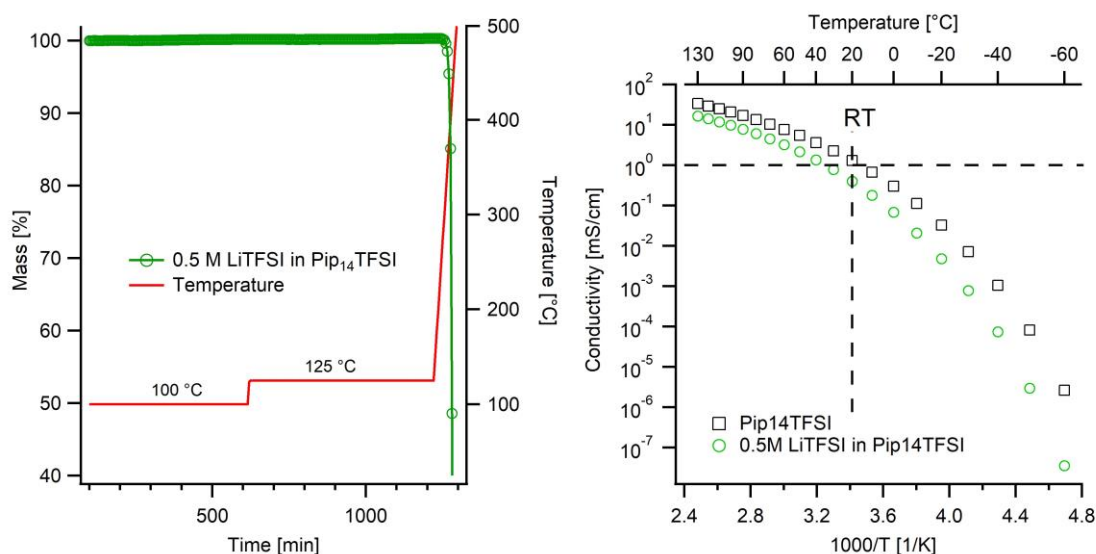


Figure 25: Long-term thermal stability and ionic conductivities of Pip₁₄TFSI and its electrolyte.

5.4 Paper IV

Ionic liquid and hybrid ionic liquid/organic electrolytes for high temperature lithium-ion battery application

While IL_{el} have many advantages, their disadvantages are high viscosities and poor transport properties. Hybrid IL/organic solvent electrolytes may resolve these shortcomings, wherefore we studied different pyrrolidinium based hybrid IL/organic solvent electrolytes for fundamental properties and application in HT-LIBs. The pure pyrrolidinium IL_{el} was studied as reference. The IL_{el} had a high thermal stability, decomposing at *ca.* 340°C, while the hybrid electrolytes showed solvent evaporation already below 100°C, setting their upper application limit < 100°C. Viscosities decreased exponentially with temperature and with the addition of the organic solvents and were around 40% lower for the hybrid electrolytes at RT (Figure 26). They all had comparable ESWs of around 5 V *vs.* Li⁺/Li⁰, with the FEC hybrid electrolyte having a *ca.* 0.5 V *vs.* Li⁺/Li⁰ lower cathodic stability than the other electrolytes, still enabling the most common cathode materials. Cycling of Li||LFP half-cells at 80°C and 1 C resulted in discharge capacities of *ca.* 160 mAh/g, which were higher than for LP30 at RT, showing a clear advantage of hybrid electrolytes at HT compared to commercial electrolytes at RT. Rate capability tests revealed a preference for the FEC hybrid electrolyte, which enabled a minor loss of 5% of the discharge capacity when moving from 1 C to 4 C, while the other showed drops of 12-23%. Long-term battery cycling at 80°C and 2 C resulted in stable cycling of the FEC hybrid electrolyte for 300 cycles, only losing 5% capacity, while the IL_{el} showed rapid capacity fading after 250 cycles (Figure 26), in further support for improved performance of hybrid electrolytes.

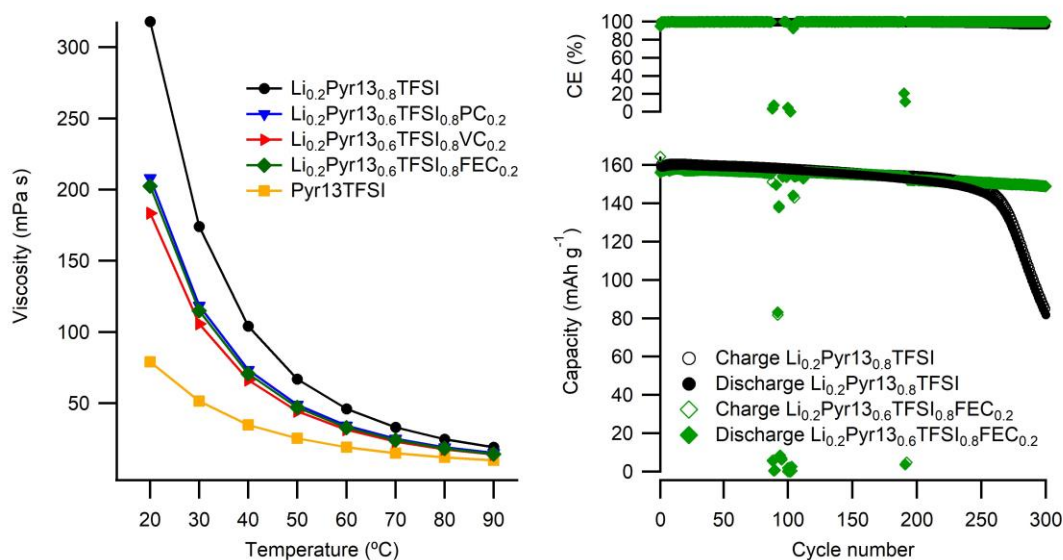


Figure 26: Viscosities and charge/discharge capacities of the electrolytes.

5.5 Paper V

Pyrrolidinium FSI and TFSI based polymerized ionic liquids as electrolytes for high temperature lithium-ion batteries

PIL_{el} unite increased ionic conductivities and high thermal stabilities of ILs with the mechanical properties of polymers, which should make them ideal for HT-LIBs. Therefore, we studied two ternary sets of PIL_{el} with different IL/Li-salt molar fraction (9:1, 6:1 and 3:1) for physical and electrochemical properties and the influence of having both TFSI and FSI anions present to elucidate any possible synergies. Set A and B both contained LiTFSI, the PDDA PIL, and the Pyr₁₄ cation, while set A exclusively contained the TFSI anion and set B both the FSI and TFSI anion. The T_g of all the PIL_{el} were low (-82 to -63°C), but higher for the PIL_{el} with increased Li-salt concentration, however, the increase was stronger for set A hinting on stronger Li⁺-TFSI interaction. Dynamic TGA showed high thermal stabilities of all PIL_{el} with set B being thermally less stable (180 vs. 350°C), which was confirmed by isothermal TGA at 125°C where set B PIL_{el} showed a mass loss while set A was stable. However, all the PIL_{el} were stable during isothermal TGA at 100°C, the ionic conductivities increased with temperature and Li-salt concentration, and almost all of the PIL_{el} had ≥ 0.1 mS/cm at 80-100°C, suggesting their general usage in HT-LIBs.

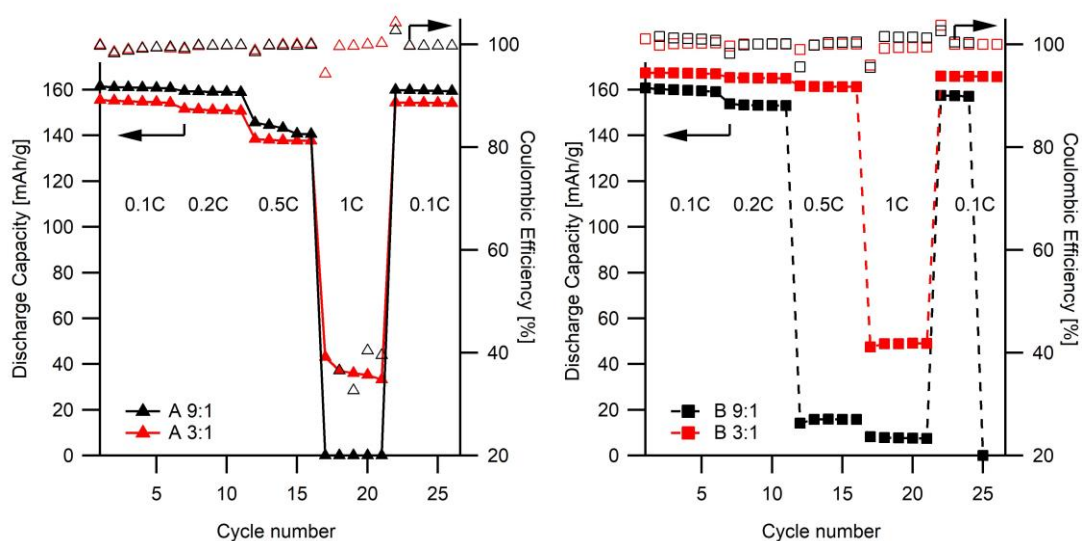


Figure 27: Cycling performance for Li|PIL_{el}|LFP cells at varying C-rates.

Anodic stabilities were higher for set B PIL_{el}, due to a synergetic effect of having both anions present, possibly enabling high voltage cathodes, while cathodic stabilities were similar for all PIL_{el}. The interfacial resistances increase over time until a plateau is reached with lower resistances upon increased Li-salt concentration, and especially for set B PIL_{el} (27 vs. 300 Ω), due to a beneficial effect of the FSI anion. Rate capability tests with Li||LFP half-cells showed a clear effect of the salt concentration on the C-rate, where for set A PIL_{el} a low LiTFSI concentration slightly improved discharge

capacities at 0.1-0.5 C, while the opposite trend was seen at 1 C, where only the PIL_{el} with a high LiTFSI concentration (A 3:1) delivered 35 mAh/g (Figure 27). For set B PIL_{el}, stable discharge capacities were reached for the PIL_{el} with high LiTFSI concentration (B 3:1), enabling 160 mAh/g even at 0.5 C and altogether resulting in the best battery cycling performance. However, this did not occur during long-term cycling at 0.5 C where B 3:1, possibly suffered from a lower SEI quality.

5.6 Paper VI

Towards more thermally stable Li-ion battery electrolytes with salts and solvents sharing nitrile functionality

HT-LIB electrolytes do not have to be IL based. Another alternative is nitrile based electrolytes, which were investigated for physical properties and performance. The electrolytes showed liquid ranges dependent on the solvents applied and extendable to slightly lower temperatures; the T_m shifted from 2°C for ADN to -20°C for the ADN:SL:EC (ASE) electrolyte, enabling extended low temperature storage and operation. All the electrolytes had rather high viscosities in the range of 12 – 20 mPa s at 20°C and only moderate ionic conductivities of *ca.* 1 mS/cm at RT. The LiTDI based electrolytes overall had the highest ionic conductivities. In terms of thermal stability, the ADN and ADN:SL (AS) electrolytes had high flash points of > 150°C and exhibited only slow solvent evaporation and no CO₂ release during the thermal analysis (Figure 28), making them the safer choices. The ternary ASE electrolytes, however, showed EC evaporation already at *ca.* 70°C and CO₂ traces at slightly higher temperatures, clearly limiting these electrolytes. For the corresponding solvent mixture without any Li-salt, no CO₂ was detected by FT-IR, suggesting a catalytic effect of the Li⁺ and/or the anion.

The performance of the Li||LFP half-cells was only moderate with discharge capacities of *ca.* 140 mAh/g, but showed relatively high coulombic efficiencies of 99.6% and 99.8% for the two AS electrolytes with LiTDI and LiDCTA, respectively, (Figure 28).

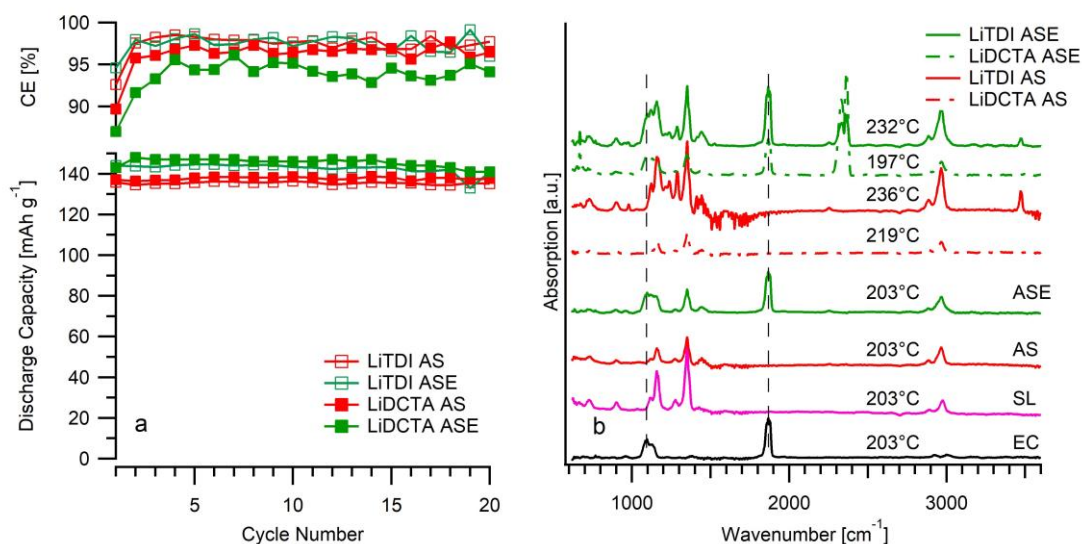


Figure 28: a) Discharge capacities for Li||LFP cells and b) TGA FT-IR spectra.

6 Conclusions and Outlook

- The quality of the LiFSI salt is highly dependent on the supplier/manufacturer and possibly originates in the synthesis process. The impurities present alter the thermal stabilities, but we have not seen any effect on cycling performance – but further, more demanding cycling, is warranted.
- IL_{el} are a viable path for HT-LIB operating at *ca.* 100°C.
- A synergetic effect of having both TFSI and FSI anions present in the electrolyte exists for a certain ratio. This results in increased thermal stabilities and high ionic conductivities. Possibly a mixed FSI and TFSI solvation of Li⁺ exists in such electrolytes.
- Even though the IL_{el} show promising properties at HT, their final viability as HT-LIB electrolytes has to be tested by cycling experiments, *etc.*
- Transport numbers should if possible be determined (for the mixed systems) to increase the understanding of the electrolytes.
- Organic solvent/IL hybrid electrolytes are very promising for HT-LIBs, outperforming conventional and IL_{el} in terms of capacity retention and long-term stability. The hybrid electrolyte performed better at 80°C than the conventional electrolyte at RT.
- Ternary PIL_{el} are promising for HT-LIBs, however, with a disadvantage in low rate capabilities. A vibrational/NMR spectroscopy study could be useful for a more detailed understanding of the Li⁺ transport mechanism and to better tailor the PIL_{el}.
- Nitrile based electrolytes need improved electrochemical performance, but exhibit promising safety features especially in the absence of EC. The latter calls for further studies on possible alternatives to EC also for conventional electrolytes.
- Further tailoring of the electrolytes can/should be possible by application of additives, *e.g.* HT stable organic or silicon based solvents. The target could be to further increase the thermal stability, enhance the ionic conductivity, or improve the SEI.

Acknowledgements

First of all, I would like to express my deepest gratitude to my supervisors Patrik and Johan for their continuous and exceptional support, their patience, their guidance and for the inspiring and motivating discussions they have had with me over the past years. I also want to thank Patrik for giving me the opportunity to do a PhD in such an interesting field.

Many thanks to the Stiftelsen för Strategisk Forskning (SSF) for enabling this project as well as for the resulting collaborations with Uppsala University and KTH. Thanks to Solveig, Kristina and Leif for our successful publication of our combined materials!

To everyone at KMF and beyond, thanks for providing a welcoming & scientific environment, where ideas can be discussed to increase the understanding in all matters. I would like to give special thanks to Muhammad for designing the front page of this thesis, many thanks! Even though there are a lot of high quality devices at KMF, from time to time *troubles* appear. For all his time, helping out, and solving problems, Ezio, thank you so much! All of us need to start at some point, and even though this is now far in the past, I would like to thank two KMF alumni members for introducing me into different measurement techniques: Maciej & Jagath, thanks a lot! To all the members of FFF, thank you for the pleasant meetings and fun events. Especially Anna, Masoud, Silvia, Pier Paolo and Edoardo.

Scientific life is interesting in so many ways, however, it can only be completely fulfilling when there is also some time to relax. Therefore, I would like to thank my friends and my family, especially Philine & little Linus for their support and encouragements.

Thanks to all of you!

Yours truly,
Manfred

Gothenburg, the 1st of November 2017

References

- [1] Intergovernmental Panel on Climate Change, (n.d.). <http://www.ipcc.ch/index.htm> (accessed September 17, 2017).
- [2] United Nations Framework Convention on Climate Change, (n.d.). <http://newsroom.unfccc.int/unfccc-newsroom/finale-cop21/> (accessed September 17, 2017).
- [3] B. Seger, Electric cars are not the key to CO₂ reduction in the automotive industry, 2017-10-11. (n.d.). <https://tinyurl.com/fuelconsumptionvehicles> (accessed October 18, 2017).
- [4] H. Ritchie et al., Energy Production & Changing Energy Sources, OurWorldInData.org. (2017). <https://ourworldindata.org/energy-production-and-changing-energy-sources/> (accessed September 28, 2017).
- [5] T.A. Boden et al., Global, Regional, and National Fossil-Fuel CO₂ Emissions, (2017). doi:10.3334/CDIAC/00001_V2017.
- [6] C. McKerracher, EV market trends and outlook, 2017. [https://www.transportenvironment.org/sites/te/files/EV market trends and outlook %28by Colin McKerracher%29.pdf](https://www.transportenvironment.org/sites/te/files/EV%20market%20trends%20and%20outlook%20by%20Colin%20McKerracher.pdf) (accessed September 28, 2017).
- [7] R. Matulka, The History of the Electric Car, (2014). <https://energy.gov/articles/history-electric-car> (accessed November 1, 2017).
- [8] T. Randall, Tesla's Model 3 Arrives With a Surprise 310-Mile Range, (2017). <https://www.bloomberg.com/news/articles/2017-07-29/tesla-s-model-3-arrives-with-a-surprise-310-mile-range> (accessed August 29, 2017).
- [9] J.B. Goodenough et al., The Li-ion rechargeable battery: A perspective, *J. Am. Chem. Soc.* 135 (2013) 1167–76. doi:10.1021/ja3091438.
- [10] B. Scrosati et al., Lithium batteries: Status, prospects and future, *J. Power Sources.* 195 (2010) 2419–2430. doi:10.1016/j.jpowsour.2009.11.048.
- [11] Greenhouse gas emission statistics, Ec.europa.eu. (2017). http://ec.europa.eu/eurostat/statistics-explained/index.php/Greenhouse_gas_emission_statistics (accessed September 28, 2017).
- [12] S.F. Lux et al., The mechanism of HF formation in LiPF₆ based organic carbonate electrolytes, *Electrochem. Commun.* 14 (2012) 47–50. doi:10.1016/j.elecom.2011.10.026.
- [13] E. Wikner, Lithium ion Battery Aging: Battery Lifetime Testing and Physics-based Modeling for Electric Vehicle Applications, Chalmers University of Technology, 2017.
- [14] T.B. Reddy, *Linden's Handbook of Batteries*, Fourth Ed., McGraw-Hill Education, 2011.
- [15] H.D. Yoo et al., On the challenge of developing advanced technologies for electrochemical energy storage and conversion, *Mater. Today.* 17 (2014) 110–121. doi:10.1016/j.mattod.2014.02.014.

- [16] X. Wang et al., Nonflammable Trimethyl Phosphate Solvent-Containing Electrolytes for Lithium-Ion Batteries: I. Fundamental Properties, *J. Electrochem. Soc.* 148 (2001) A1058. doi:10.1149/1.1397773.
- [17] H. Ota et al., Effect of cyclic phosphate additive in non-flammable electrolyte, *J. Power Sources.* 119–121 (2003) 393–398. doi:10.1016/S0378-7753(03)00259-3.
- [18] H. Nakagawa et al., Application of nonflammable electrolyte with room temperature ionic liquids (RTILs) for lithium-ion cells, *J. Power Sources.* 174 (2007) 1021–1026. doi:10.1016/j.jpowsour.2007.06.133.
- [19] F. Endres et al., Air and water stable ionic liquids in physical chemistry, *Phys. Chem. Chem. Phys.* 8 (2006) 2101–16. doi:10.1039/b600519p.
- [20] S. Aparicio et al., Thermophysical Properties of Pure Ionic Liquids: Review of Present Situation, *Ind. Eng. Chem. Res.* 49 (2010) 9580–9595. doi:10.1021/ie101441s.
- [21] M. Armand et al., Ionic-liquid materials for the electrochemical challenges of the future, *Nat. Mater.* 8 (2009) 621–9. doi:10.1038/nmat2448.
- [22] A. Matic et al., Ionic liquids for energy applications, *MRS Bull.* 38 (2013) 533–537. doi:10.1557/mrs.2013.154.
- [23] M. Montanino et al., Mixed organic compound-ionic liquid electrolytes for lithium battery electrolyte systems, *J. Power Sources.* 269 (2014) 608–615. doi:10.1016/j.jpowsour.2014.07.027.
- [24] A.S. Shaplov et al., Recent Advances in Innovative Polymer Electrolytes based on Poly(ionic liquid)s, *Electrochim. Acta.* 175 (2015) 18–34. doi:10.1016/j.electacta.2015.03.038.
- [25] A.-L. Pont et al., Pyrrolidinium-based polymeric ionic liquids as mechanically and electrochemically stable polymer electrolytes, *J. Power Sources.* 188 (2009) 558–563. doi:10.1016/j.jpowsour.2008.11.115.
- [26] R.M. Dell, *Aqueous Electrolyte Batteries*, *R. Soc. Publ.* 354 (1996) 1515–1527.
- [27] G.E. Blomgren, The Development and Future of Lithium Ion Batteries, *J. Electrochem. Soc.* 164 (2017) A5019–A5025. doi:10.1149/2.0251701jes.
- [28] B. Zhang et al., A superior thermostable and nonflammable composite membrane towards high power battery separator, *Nano Energy.* 10 (2014) 277–287. doi:10.1016/j.nanoen.2014.10.001.
- [29] H. Berg, *Batteries for Electric Vehicles*, 1st ed., Cambridge University Press, 2015.
- [30] N. Sridhar, Driving the future of HEV / EV with high-voltage solutions, 2017. <http://www.tij.co.jp/jp/lit/wp/slyy052a/slyy052a.pdf> (accessed November 1, 2017).
- [31] F. Lambert, Teardown of new 100 kWh Tesla battery pack reveals new cooling system and 102 kWh capacity, (2017). <https://electrek.co/2017/01/24/tesla-teardown-100-kwh-battery-pack/> (accessed October 19, 2017).
- [32] B. Scrosati, History of lithium batteries, *J. Solid State Electrochem.* 15 (2011) 1623–1630. doi:10.1007/s10008-011-1386-8.

- [33] K. Brandt, Historical development of secondary lithium batteries, *Solid State Ionics*. 69 (1994) 173–183.
- [34] T. Ohzuku, Formation of Lithium-Graphite Intercalation Compounds in Nonaqueous Electrolytes and Their Application as a Negative Electrode for a Lithium Ion (Shuttlecock) Cell, *J. Electrochem. Soc.* 140 (1993) 2490. doi:10.1149/1.2220849.
- [35] B. Scrosati, Lithium Rocking Chair Batteries: An Old Concept?, *J. Electrochem. Soc.* 139 (1992) 2776–2781.
- [36] T. Ohzuku et al., Innovative insertion material of $\text{LiAl}_{1/4}\text{Ni}_{3/4}\text{O}_2$ (R3m) for lithium-ion (shuttlecock) batteries, *J. Power Sources*. 68 (1997) 131–134. doi:10.1016/S0378-7753(97)02516-0.
- [37] R. Fong, Studies of Lithium Intercalation into Carbons Using Nonaqueous Electrochemical Cells, *J. Electrochem. Soc.* 137 (1990) 2009. doi:10.1149/1.2086855.
- [38] B. Diouf et al., Potential of lithium-ion batteries in renewable energy, *Renew. Energy*. 76 (2015) 375–380. doi:10.1016/j.renene.2014.11.058.
- [39] Groupe Bolloré, Blue solutions business report 2013, 2013. <https://www.blue-solutions.com/en/blue-solutions/investisseurs/informations-reglementees/> (accessed November 1, 2017).
- [40] Autolib', A unique technology for smart energy management, 2017. (n.d.). <https://www.autolib.eu/en/our-commitment/bluecar-menu-en/100-electric/> (accessed November 1, 2017).
- [41] K. Xu, Electrolytes and interphases in li-ion batteries and beyond., *Chem. Rev.* 114 (2014) 11503–618. doi:10.1021/cr500003w.
- [42] W. Li et al., Inhibition of solid electrolyte interface formation on cathode particles for lithium-ion batteries, *J. Power Sources*. 168 (2007) 258–264. doi:10.1016/j.jpowsour.2007.02.055.
- [43] J. Guo et al., A novel $\text{Li}_4\text{Ti}_5\text{O}_{12}$ -based high-performance lithium-ion electrode at elevated temperature, *J. Mater. Chem. A*. 3 (2015) 4938–4944. doi:10.1039/C4TA05660D.
- [44] F. Mestre-Aizpurua et al., High temperature lithium cells using conversion oxide electrodes, *J. Appl. Electrochem.* 40 (2010) 1365–1370. doi:10.1007/s10800-010-0103-0.
- [45] S. Megahed et al., Lithium-ion rechargeable batteries, *J. Power Sources*. 51 (1994) 79–104. doi:10.1016/0378-7753(94)01956-8.
- [46] K. Sawai et al., Carbon materials for lithium-ion (shuttlecock) cells, *Solid State Ionics*. 69 (1994) 273–283. doi:10.1016/0167-2738(94)90416-2.
- [47] J.R. Dahn et al., Mechanisms for Lithium Insertion in Carbonaceous Materials, *Science* 270 (1995) 590–593. doi:10.1126/science.270.5236.590.
- [48] N. Nitta et al., Li-ion battery materials: Present and future, *Mater. Today*. 18 (2015) 252–264. doi:10.1016/j.mattod.2014.10.040.

- [49] Y.S. Park et al., Effects of particle size on the thermal stability of lithiated graphite anode, *Electrochim. Acta.* 54 (2009) 3339–3343. doi:10.1016/j.electacta.2008.12.030.
- [50] B. Zhao et al., A comprehensive review of $\text{Li}_4\text{Ti}_5\text{O}_{12}$ -based electrodes for lithium-ion batteries: The latest advancements and future perspectives, *Mater. Sci. Eng. R Reports.* 98 (2015) 1–71. doi:10.1016/j.mser.2015.10.001.
- [51] K. Zaghbi et al., Safe and fast-charging Li-ion battery with long shelf life for power applications, *J. Power Sources.* 196 (2011) 3949–3954. doi:10.1016/j.jpowsour.2010.11.093.
- [52] S. Menne et al., The influence of the electrochemical and thermal stability of mixtures of ionic liquid and organic carbonate on the performance of high power lithium-ion batteries, *Electrochim. Acta.* 90 (2013) 641–648. doi:10.1016/j.electacta.2012.12.042.
- [53] M. Kamata et al., Application of Neutron Radiography to Visualize the Motion of Lithium Ions in Lithium-Ion Conducting Materials, *Electrochem. Soc.* 143 (1996) 1866–1870.
- [54] U. Kasavajjula et al., Nano- and bulk-silicon-based insertion anodes for lithium-ion secondary cells, *J. Power Sources.* 163 (2007) 1003–1039. doi:10.1016/j.jpowsour.2006.09.084.
- [55] L. Wu et al., Silicon nanoparticles embedded in a porous carbon matrix as a high-performance anode for lithium-ion batteries, *J. Mater. Chem. A.* 4 (2016) 11381–11387. doi:10.1039/C6TA04398D.
- [56] M. Winter et al., Electrochemical lithiation of tin and tin-based intermetallics and composites, *Electrochim. Acta.* 45 (1999) 31–50. doi:10.1016/S0013-4686(99)00191-7.
- [57] A. Casimir et al., Silicon-based anodes for lithium-ion batteries: Effectiveness of materials synthesis and electrode preparation, *Nano Energy.* 27 (2016) 359–376. doi:10.1016/j.nanoen.2016.07.023.
- [58] X. Zhou et al., Self-assembled nanocomposite of silicon nanoparticles encapsulated in graphene through electrostatic attraction for lithium-ion batteries, *Adv. Energy Mater.* 2 (2012) 1086–1090. doi:10.1002/aenm.201200158.
- [59] J. Chang et al., Multilayered Si nanoparticle/reduced graphene oxide hybrid as a high-performance lithium-ion battery anode, *Adv. Mater.* 26 (2014) 758–764. doi:10.1002/adma.201302757.
- [60] Y. Chen et al., Firmly bonded graphene-silicon nanocomposites as high-performance anode materials for lithium-ion batteries, *RSC Adv.* 5 (2015) 46173–46180. doi:10.1039/c5ra05869d.
- [61] T. Ohzuku et al., Why transition metal (di) oxides are the most attractive materials for batteries, *Solid State Ionics.* 69 (1994) 201–211. doi:10.1016/0167-2738(94)90410-3.
- [62] M.M. Thackeray, Lithiated Oxides for Lithium Ion Batteries, *J. Electrochem. Soc.* 142 (1995) 2558–2563.

- [63] M.K. Aydinol et al., First-Principles Prediction of Insertion Potentials in Li-Mn Oxides for Secondary Li Batteries, *J. Electrochem. Soc.* 144 (1997) 3832. doi:10.1149/1.1838099.
- [64] A.K. Padhi et al., Effect of Structure on the Fe³⁺/Fe²⁺ Redox Couple in Iron Phosphates, *Electrochem. Soc.* 144 (1997) 1609–1613.
- [65] Z. Zhang et al., *Rechargeable Batteries*, Springer International Publishing, Cham, 2015. doi:10.1007/978-3-319-15458-9.
- [66] B. Wu et al., LiFePO₄ Cathode Material, *Electr. Veh. - Benefits Barriers*. (2011) 199–216. doi:10.5772/717.
- [67] D. Doughty et al., A General Discussion of Li Ion Battery Safety, *Electrochem. Soc. Interface*. (2012) 37–44. doi:10.1021/cm901452z.
- [68] M.J. Lee et al., High performance LiMn₂O₄ cathode materials grown with epitaxial layered nanostructure for Li-Ion batteries, *Nano Lett.* 14 (2014) 993–999. doi:10.1021/nl404430e.
- [69] G.E. Blomgren, Electrolytes for advanced batteries, *J. Power Sources*. 81–82 (1999) 112–118. doi:10.1016/S0378-7753(99)00188-3.
- [70] J. Tarascon et al., New electrolyte compositions stable over the 0 to 5 V voltage range and compatible with the Li_{1+x}Mn₂O₄/carbon Li-ion cells, *Solid State Ionics*. 69 (1994) 293–305. doi:10.1016/0167-2738(94)90418-9.
- [71] J.M. Tarascon et al., Issues and challenges facing rechargeable lithium batteries, *Nature*. 414 (2001) 359–367. <http://www.ncbi.nlm.nih.gov/pubmed/11713543>.
- [72] J. Xia et al., Enabling linear alkyl carbonate electrolytes for high voltage Li-ion cells, *J. Power Sources*. 328 (2016) 124–135. doi:10.1016/j.jpowsour.2016.08.015.
- [73] S.-K. Jeong et al., Surface Film Formation on Graphite Negative Electrode in Lithium-Ion Batteries: AFM Study in an Ethylene Carbonate-Based Solution, *J. Electrochem. Soc.* 148 (2001) A989. doi:10.1149/1.1387981.
- [74] E. Peled et al., Review—SEI: Past, Present and Future, *J. Electrochem. Soc.* 164 (2017) A1703–A1719. doi:10.1149/2.1441707jes.
- [75] E. Peled, The Electrochemical Behavior of Alkali and Alkaline Earth Metals in Nonaqueous Battery Systems—The Solid Electrolyte Interphase Model, *J. Electrochem. Soc.* 126 (1979) 2047. doi:10.1149/1.2128859.
- [76] A. Du Pasquier, Differential Scanning Calorimetry Study of the Reactivity of Carbon Anodes in Plastic Li-Ion Batteries, *J. Electrochem. Soc.* 145 (1998) 472. doi:10.1149/1.1838287.
- [77] A.M. Andersson et al., Chemical Composition and Morphology of the Elevated Temperature SEI on Graphite, *J. Electrochem. Soc.* 148 (2001) A1100. doi:10.1149/1.1397771.
- [78] K. Edström et al., The cathode-electrolyte interface in the Li-ion battery, *Electrochim. Acta*. 50 (2004) 397–403. doi:10.1016/j.electacta.2004.03.049.

- [79] S. Theivaprakasam et al., Electrochemical studies of N-Methyl N-Propyl Pyrrolidinium bis(trifluoromethanesulfonyl) imide ionic liquid mixtures with conventional electrolytes in LiFePO₄/Li cells, *Electrochim. Acta.* 180 (2015) 737–745. doi:10.1016/j.electacta.2015.08.137.
- [80] J.T. Dudley et al., Conductivity of electrolytes for rechargeable lithium batteries, *J. Power Sources.* 35 (1991) 59–82. doi:10.1016/0378-7753(91)80004-H.
- [81] S.S. Zhang et al., Aluminum corrosion in electrolyte of Li-ion battery, *J. Power Sources.* 109 (2002) 458–464.
- [82] M. Schmidt et al., Lithium fluoroalkylphosphates: A new class of conducting salts for electrolytes for high energy lithium-ion batteries, *J. Power Sources.* 97–98 (2001) 557–560. doi:10.1016/S0378-7753(01)00640-1.
- [83] E. Peled, An Advanced Tool for the Selection of Electrolyte Components for Rechargeable Lithium Batteries, *J. Electrochem. Soc.* 145 (1998) 3482. doi:10.1149/1.1838831.
- [84] S.E. Sloop et al., Chemical Reactivity of PF₅ and LiPF₆ in Ethylene Carbonate/Dimethyl Carbonate Solutions, *Electrochem. Solid-State Lett.* 4 (2001) A42–A44. doi:10.1149/1.1353158.
- [85] I.A. Shkrob et al., Allotropic Control: How Certain Fluorinated Carbonate Electrolytes Protect Aluminum Current Collectors by Promoting the Formation of Insoluble Coordination Polymers, *J. Phys. Chem. C.* 120 (2016) 18435–18444. doi:10.1021/acs.jpcc.6b05241.
- [86] U. Heider et al., Challenge in manufacturing electrolyte solutions for lithium and lithium ion batteries quality control and minimizing contamination level, *J. Power Sources.* 81–82 (1999) 119–122. doi:10.1016/S0378-7753(99)00142-1.
- [87] Y. Xia et al., Capacity Fading on Cycling of 4 V Li/LiMn₂O₄ Cells, *J. Electrochem. Soc.* 144 (1997) 2593. doi:10.1149/1.1837870.
- [88] Z. Chen et al., LiPF₆/LiBOB blend salt electrolyte for high-power lithium-ion batteries, *Electrochim. Acta.* 51 (2006) 3322–3326. doi:10.1016/j.electacta.2005.09.027.
- [89] A.M. Andersson et al., The influence of lithium salt on the interfacial reactions controlling the thermal stability of graphite anodes, *Electrochim. Acta.* 47 (2002) 1885–1898. doi:10.1016/S0013-4686(02)00044-0.
- [90] K. Zaghbi et al., An improved high-power battery with increased thermal operating range: C-LiFePO₄/C-Li₄Ti₅O₁₂, *J. Power Sources.* 216 (2012) 192–200. doi:10.1016/j.jpowsour.2012.05.025.
- [91] M. Dahbi et al., Comparative study of EC/DMC LiTFSI and LiPF₆ electrolytes for electrochemical storage, *J. Power Sources.* 196 (2011) 9743–9750. doi:10.1016/j.jpowsour.2011.07.071.
- [92] L.J. Krause et al., Corrosion of aluminum at high voltages in non-aqueous electrolytes containing perfluoroalkylsulfonyl imides; new lithium salts for lithium-ion cells, *J. Power Sources.* 68 (1997) 320–325. doi:10.1016/S0378-7753(97)02517-2.

- [93] M. Morita et al., Anodic behavior of aluminum in organic solutions with different electrolytic salts for lithium ion batteries, *Electrochim. Acta.* 47 (2002) 2787–2793. doi:[http://dx.doi.org/10.1016/S0013-4686\(02\)00164-0](http://dx.doi.org/10.1016/S0013-4686(02)00164-0).
- [94] L. Péter et al., Anodic dissolution of aluminium in organic electrolytes containing perfluoroalkylsulfonyl imides, *J. Appl. Electrochem.* 29 (1999) 1053–1061. doi:[10.1023/A:1003573430989](https://doi.org/10.1023/A:1003573430989).
- [95] X. Chen et al., Mixed salts of LiTFSI and LiBOB for stable LiFePO₄-based batteries at elevated temperatures, *J. Mater. Chem. A.* 2 (2014) 2346. doi:[10.1039/c3ta13043f](https://doi.org/10.1039/c3ta13043f).
- [96] K. Matsumoto et al., Suppression of aluminum corrosion by using high concentration LiTFSI electrolyte, *J. Power Sources.* 231 (2013) 234–238. doi:[10.1016/j.jpowsour.2012.12.028](https://doi.org/10.1016/j.jpowsour.2012.12.028).
- [97] D. Di Censo et al., Non-corrosive electrolyte compositions containing perfluoroalkylsulfonyl imides for high power Li-ion batteries, *Electrochem. Commun.* 7 (2005) 1000–1006. doi:<http://dx.doi.org/10.1016/j.elecom.2005.07.005>.
- [98] B. Garcia et al., Room temperature molten salts as lithium battery electrolyte, *Electrochim. Acta.* 49 (2004) 4583–4588. doi:[10.1016/j.electacta.2004.04.041](https://doi.org/10.1016/j.electacta.2004.04.041).
- [99] B. Garcia et al., Aluminium corrosion in room temperature molten salt, *J. Power Sources.* 132 (2004) 206–208. doi:[10.1016/j.jpowsour.2003.12.046](https://doi.org/10.1016/j.jpowsour.2003.12.046).
- [100] E. Paillard et al., Electrochemical and Physicochemical Properties of PY₁₄FSI-Based Electrolytes with LiFSI, *J. Electrochem. Soc.* 156 (2009) A891–A895. doi:[10.1149/1.3208048](https://doi.org/10.1149/1.3208048).
- [101] L. Li et al., Transport and Electrochemical Properties and Spectral Features of Non-Aqueous Electrolytes Containing LiFSI in Linear Carbonate Solvents, *J. Electrochem. Soc.* 158 (2011) A74–A82. doi:[10.1149/1.3514705](https://doi.org/10.1149/1.3514705).
- [102] Y. Deguchi et al., An advanced ionic liquid-lithium salt electrolyte mixture based on the bis(fluoromethanesulfonyl)imide anion, *Electrochem. Commun.* 43 (2014) 5–8. doi:[10.1016/j.elecom.2014.02.017](https://doi.org/10.1016/j.elecom.2014.02.017).
- [103] H.-B. Han et al., Lithium bis(fluorosulfonyl)imide (LiFSI) as conducting salt for nonaqueous liquid electrolytes for lithium-ion batteries: Physicochemical and electrochemical properties, *J. Power Sources.* 196 (2011) 3623–3632. doi:[10.1016/j.jpowsour.2010.12.040](https://doi.org/10.1016/j.jpowsour.2010.12.040).
- [104] B. Philippe et al., Improved performance of nano-silicon electrodes using the salt LiFSI – A photoelectron spectroscopy study, *J. Am. Chem. Soc.* 135 (2013) 9829–9842. doi:[10.1021/ja403082s](https://doi.org/10.1021/ja403082s).
- [105] M. Nie et al., Role of Lithium Salt on Solid Electrolyte Interface (SEI) Formation and Structure in Lithium Ion Batteries, *J. Electrochem. Soc.* 161 (2014) A1001–A1006. doi:[10.1149/2.054406jes](https://doi.org/10.1149/2.054406jes).
- [106] K. Kubota et al., Novel inorganic ionic liquids possessing low melting temperatures and wide electrochemical windows: Binary mixtures of alkali bis(fluorosulfonyl)amides, *Electrochem. Commun.* 10 (2008) 1886–1888. doi:[10.1016/j.elecom.2008.10.001](https://doi.org/10.1016/j.elecom.2008.10.001).

- [107] S. Shui Zhang, An unique lithium salt for the improved electrolyte of Li-ion battery, *Electrochem. Commun.* 8 (2006) 1423–1428. doi:10.1016/j.elecom.2006.06.016.
- [108] U. Wietelmann et al., Lithium bisoxalatoborate, the production thereof and its use as a conducting salt, US 6,506,516 B1, 1999.
- [109] K. Xu et al., Lithium Bis(oxalato)borate Stabilizes Graphite Anode in Propylene Carbonate, *Electrochem. Solid-State Lett.* 5 (2002) A259–A262.
- [110] K. Xu et al., LiBOB: Is it an alternative salt for lithium ion chemistry?, *J. Power Sources.* 146 (2005) 79–85. doi:10.1016/j.jpowsour.2005.03.153.
- [111] X. Zhang et al., Passivation of Aluminum in Lithium-Ion Battery Electrolytes with LiBOB, *J. Electrochem. Soc.* 153 (2006) B365. doi:10.1149/1.2218269.
- [112] K. Xu, Tailoring Electrolyte Composition for LiBOB, *J. Electrochem. Soc.* 155 (2008) A733. doi:10.1149/1.2961055.
- [113] M. Armand et al., Pentacyclic anion salt and use thereof as an electrolyte, US 8,927,160 B2, 2015.
- [114] L. Niedzicki et al., New Covalent Salts of the 4+ V Class For Li Batteries, *J. Power Sources.* 196 (2011) 8696–8700. doi:10.1016/j.jpowsour.2011.06.030.
- [115] J. Scheers et al., All fluorine-free lithium battery electrolytes, *J. Power Sources.* 251 (2014) 451–458. doi:10.1016/j.jpowsour.2013.11.042.
- [116] M. Kerner et al., Towards more thermally stable Li-ion battery electrolytes with salts and solvents sharing nitrile functionality, *J. Power Sources.* 332 (2016) 204–212. doi:10.1016/j.jpowsour.2016.09.101.
- [117] W.A. Henderson, Nonaqueous Electrolytes: Advances in Lithium Salts, in: R. Jow, K. Xu, O. Borodin, M. Ue (Eds.), *Electrolytes Lithium Lithium-Ion Batter.*, Springer, 2014: pp. 1–92.
- [118] C. Reichardt et al., Production methods, properties, and main applications, in: *Handb. Solvents*, Second Edi, Elsevier, 2014: pp. 73–116. doi:10.1016/B978-1-895198-64-5.50005-2.
- [119] H.V. Venkatesetty, *Electrolytes for rechargeable lithium batteries*, Elsevier Ltd., 1989. doi:10.1109/IECEC.1989.74696.
- [120] S. Hess et al., Flammability of Li-Ion Battery Electrolytes: Flash Point and Self-Extinguishing Time Measurements, *J. Electrochem. Soc.* 162 (2015) A3084–A3097. doi:10.1149/2.0121502jes.
- [121] K. Xu et al., Evaluation of Fluorinated Alkyl Phosphates as Flame Retardants in Electrolytes for Li-Ion Batteries: II. Performance in Cell, *J. Electrochem. Soc.* 150 (2003) A170. doi:10.1149/1.1533041.
- [122] R.-S. Kühnel et al., Mixtures of ionic liquid and organic carbonate as electrolyte with improved safety and performance for rechargeable lithium batteries, *Electrochim. Acta.* 56 (2011) 4092–4099. doi:10.1016/j.electacta.2011.01.116.
- [123] C. Daniel et al., *Handbook of Battery Materials*, 2nd ed., Wiley-VCH Verlag GmbH, 2011.

- [124] Vinylene carbonate, (n.d).
http://www.chemicalbook.com/ChemicalProductProperty_EN_CB9119200.htm
(accessed October 2, 2017).
- [125] Y. Abu-Lebdeh et al., High-Voltage Electrolytes Based on Adiponitrile for Li-Ion Batteries, *J. Electrochem. Soc.* 156 (2009) A60. doi:10.1149/1.3023084.
- [126] P. Isken et al., High flash point electrolyte for use in lithium-ion batteries, *Electrochim. Acta.* 56 (2011) 7530–7535. doi:10.1016/j.electacta.2011.06.095.
- [127] A. Hofmann et al., Anodic Aluminum Dissolution of LiTFSA Containing Electrolytes for Li-Ion-Batteries, *Electrochim. Acta.* 116 (2014) 388–395. doi:10.1016/j.electacta.2013.11.085.
- [128] M. Ohtake et al., Physical Properties of Fluorinated Cyclic Carbonates for Secondary Lithium Batteries, *Electrochem. Soc.* 802 (2008) 175.
- [129] Chemical Book, (n.d.).
http://www.chemicalbook.com/ChemicalProductProperty_EN_CB9420252.htm
(accessed October 28, 2017).
- [130] MSDS solutions center, (n.d.). <http://www.msds.com/> (accessed October 28, 2017).
- [131] T. Achiha et al., Thermal Stability and Electrochemical Properties of Fluorine Compounds as Nonflammable Solvents for Lithium-Ion Batteries, *J. Electrochem. Soc.* 157 (2010) A707. doi:10.1149/1.3377084.
- [132] M.C. Smart et al., Improved performance of lithium-ion cells with the use of fluorinated carbonate-based electrolytes, *J. Power Sources.* 119–121 (2003) 359–367. doi:10.1016/S0378-7753(03)00266-0.
- [133] J. Xiang et al., High voltage and safe electrolytes based on ionic liquid and sulfone for lithium-ion batteries, *J. Power Sources.* 233 (2013) 115–120. doi:10.1016/j.jpowsour.2013.01.123.
- [134] K.E. Johnson, What's an Ionic Liquid?, *Electrochem. Soc.* (2007) 38–41.
- [135] K.R. Seddon, A taste of the future, *Nat. Mater.* 6 (2003) 363–366.
- [136] S. Gabriel et al., Ueber einige Abkömmlinge des Propylamins, *Berichte Der Dtsch. Chem. Gesellschaft.* 21 (1888) 2669–2679. doi:10.1002/cber.18880210288.
- [137] P. Walden, Ueber die Molekulargrösse und elektrische Leitfähigkeit einiger geschmolzenen Salze, *Bull. Acad. Imper. Sci.* 1 (1914) 405–422.
- [138] J.D. Holbrey et al., Ionic Liquids, *Clean Technol. Environ. Policy.* 1 (1999) 223–236. doi:10.1007/s100980050036.
- [139] K.R. Seddon, Ionic Liquids for Clean Technology, *J. Chem. Technol. Biotechnol.* 68 (1997) 351–356.
- [140] M.J. Earle et al., Ionic liquids. Green solvents for the future, *Pure Appl. Chem.* 72 (2000) 1391–1398. doi:10.1351/pac200072071391.

- [141] V. Pejaković et al., Influence of temperature on tribological behaviour of ionic liquids as lubricants and lubricant additives, *Lubr. Sci.* 26 (2014) 107–115. doi:10.1002/lis.1233.
- [142] P.M. Dean et al., Exploring an anti-crystal engineering approach to the preparation of pharmaceutically active ionic liquids, *Cryst. Growth Des.* 9 (2009) 1137–1145. doi:10.1021/cg8009496.
- [143] W. Kubo et al., Quasi-solid-state dye-sensitized solar cells using room temperature molten salts and a low molecular weight gelator, *Chem. Commun. (Camb)*. (2002) 374–375. doi:10.1039/b110019j.
- [144] Q. Zhang et al., Recent advances in ionic liquid catalysis, *Green Chem.* 13 (2011) 2619. doi:10.1039/c1gc15334j.
- [145] H.L. Ngo et al., Thermal properties of imidazolium ionic liquids, *Thermochim. Acta.* 357–358 (2000) 97–102. doi:10.1016/S0040-6031(00)00373-7.
- [146] B. Baek et al., Pyrrolidinium cation-based ionic liquids with different functional groups: Butyl, butyronitrile, pentenyl, and methyl butyrate, *Int. J. Electrochem. Sci.* 6 (2011) 6220–6234.
- [147] G.G. Eshetu et al., Comprehensive insights into the thermal stability, biodegradability and combustion chemistry of Pyrrolidinium-based Ionic Liquids, *ChemSusChem*. (n.d.). doi:10.1002/cssc.201701006.
- [148] Y. Cao et al., Comprehensive Investigation on the Thermal Stability of 66 Ionic Liquids by Thermogravimetric Analysis, *Ind. Eng. Chem. Res.* 53 (2014) 8651–8664. doi:10.1021/ie5009597.
- [149] M. Montanino et al., The role of the cation aliphatic side chain length in piperidinium bis(trifluoromethanesulfonyl)imide ionic liquids, *Electrochim. Acta.* 57 (2011) 153–159. doi:10.1016/j.electacta.2011.03.089.
- [150] K. Kim et al., Effect of alkyl-chain length of imidazolium based ionic liquid on ion conducting and interfacial properties of organic electrolytes, *J. Ind. Eng. Chem.* 26 (2015) 136–142. doi:10.1016/j.jiec.2014.11.025.
- [151] D.M. Fox et al., Flammability and Thermal Analysis Characterization of Imidazolium-Based Ionic Liquids, *Ind. Eng. Chem. Res.* 47 (2008) 6327–6332. doi:10.1021/ie800665u.
- [152] CoorsTek, CoorsTek, (n.d.). <https://coorstekchem.com/sites/default/files/IolyteP2-DataSheet.pdf> (accessed November 3, 2015).
- [153] CoorsTek, CoorsTek, (n.d.). https://coorstekchem.com/sites/default/files/IolyteP1-EMIM_TFSI_DataSheet.pdf (accessed November 3, 2015).
- [154] H. Weingärtner, The static dielectric permittivity of ionic liquids, *J. Mol. Liq.* 192 (2014) 185–190. doi:10.1016/j.molliq.2013.07.020.
- [155] M. Montanino et al., Physical and electrochemical properties of binary ionic liquid mixtures: (1-x) PYR₁₄TFSI-(x) PYR₁₄IM₁₄, *Electrochim. Acta.* 60 (2012) 163–169. doi:10.1016/j.electacta.2011.11.030.

- [156] M. Nádherná et al., Lithium bis(fluorosulfonyl)imide–PYR₁₄TFSI ionic liquid electrolyte compatible with graphite, *J. Power Sources*. 196 (2011) 7700–7706. doi:10.1016/j.jpowsour.2011.04.033.
- [157] G.B. Appetecchi et al., Ionic liquid-based electrolytes for high energy, safer lithium batteries, *ACS Symp. Ser.* 1117 (2012) 67–128. doi:10.1021/bk-2012-1117.ch004.
- [158] J.C. Salamone et al., Synthesis and homopolymerization studies of vinylimidazolium salts, *Polymer* 14 (1973) 639–644.
- [159] H. Ohno et al., Room-Temperature Molten Salt Polymers as a Matrix for Fast Ion Conduction, *Chem. Lett.* 27 (1998) 751–752. doi:/doi.org/10.1246/cl.1998.751.
- [160] H. Yu et al., Poly(Ionic Liquid)s as Ionic Liquid-Based Innovative Polyelectrolytes, in: D. Mecerreyes (Ed.), Springer Berlin Heidelberg, Berlin, Heidelberg, 2015: pp. 153–198. doi:10.1007/978-3-662-44903-5.
- [161] J. Kadokawa, Polymerizable ionic liquids: Development to photo functional poly(ionic liquid) materials, *Tcmail*. (n.d.) 2–6.
- [162] D. Mecerreyes, Polymeric ionic liquids: Broadening the properties and applications of polyelectrolytes, *Prog. Polym. Sci.* 36 (2011) 1629–1648. doi:10.1016/j.progpolymsci.2011.05.007.
- [163] N. Matsumi et al., Polymerized ionic liquids via hydroboration polymerization as single ion conductive polymer electrolytes, *Macromolecules*. 39 (2006) 6924–6927. doi:10.1021/ma060472j.
- [164] W. Ogihara et al., Effect of cation structure on the electrochemical and thermal properties of ion conductive polymers obtained from polymerizable ionic liquids, *Electrochim. Acta*. 51 (2006) 2614–2619. doi:10.1016/j.electacta.2005.07.043.
- [165] Y. Ye et al., Anion exchanged polymerized ionic liquids: High free volume single ion conductors, *Polymer (Guildf)*. 52 (2011) 1309–1317. doi:10.1016/j.polymer.2011.01.031.
- [166] F. Fan et al., Effect of Molecular Weight on the Ion Transport Mechanism in Polymerized Ionic Liquids, *Macromolecules*. 49 (2016) 4557–4570. doi:10.1021/acs.macromol.6b00714.
- [167] V. Delhorbe et al., Unveiling the Ion Conduction Mechanism in Imidazolium-Based Poly(ionic liquids): A Comprehensive Investigation of the Structure-to-Transport Interplay, *Macromolecules*. 50 (2017) 4309–4321. doi:10.1021/acs.macromol.7b00197.
- [168] S. Mogurampelly et al., Mechanisms Underlying Ion Transport in Polymerized Ionic Liquids, (2017) 3–6. doi:10.1021/jacs.7b05579.
- [169] H. Nakajima et al., Preparation of thermally stable polymer electrolytes from imidazolium-type ionic liquid derivatives, *Polymer (Guildf)*. 46 (2005) 11499–11504. doi:10.1016/j.polymer.2005.10.005.
- [170] H. Zhang et al., Polymeric ionic liquids based on ether functionalized ammoniums and perfluorinated sulfonimides, *Polym. (United Kingdom)*. 55 (2014) 3339–3348. doi:10.1016/j.polymer.2014.03.041.

- [171] J.B. Goodenough et al., Challenges for Rechargeable Li Batteries, *Chem. Mater.* 22 (2010) 587–603. doi:10.1021/cm901452z.
- [172] A. Lewandowski et al., Ionic liquids as electrolytes for Li-ion batteries—An overview of electrochemical studies, *J. Power Sources.* 194 (2009) 601–609. doi:10.1016/j.jpowsour.2009.06.089.
- [173] S. Tsuzuki et al., Origin of the Low-Viscosity of [emim][(FSO₂)₂N] Ionic Liquid and Its Lithium Salt Mixture: Experimental and Theoretical Study of Self-Diffusion Coefficients, Conductivities, and Intermolecular Interactions, *J. Phys. Chem. B.* 114 (2010) 16329–16336. doi:10.1021/jp106870v.
- [174] D.R. MacFarlane et al., On the concept of ionicity in ionic liquids, *Phys. Chem. Chem. Phys.* 11 (2009) 4962–7. doi:10.1039/b900201d.
- [175] C. Austen Angell et al., Ionic Liquids: Past, present and future, *Faraday Discuss.* 154 (2012) 9. doi:10.1039/c1fd00112d.
- [176] C.A. Angell et al., Parallel developments in aprotic and protic ionic liquids: Physical chemistry and applications, *Acc. Chem. Res.* 40 (2007) 1228–1236. doi:10.1021/ar7001842.
- [177] N. Bucher et al., A novel ionic liquid for Li ion batteries – uniting the advantages of guanidinium and piperidinium cations, *RSC Adv.* 4 (2014) 1996–2003. doi:10.1039/c3ra46118a.
- [178] D.J. Tao et al., Low-viscosity tetramethylguanidinium-based ionic liquids with different phenolate anions: Synthesis, characterization, and physical properties, *J. Chem. Eng. Data.* 59 (2014) 4031–4038. doi:10.1021/je500631j.
- [179] T. Frömling et al., Enhanced lithium transference numbers in ionic liquid electrolytes, *J. Phys. Chem. B.* 112 (2008) 12985–90. doi:10.1021/jp804097j.
- [180] O. Borodin et al., Li⁺ Cation Environment, Transport, and Mechanical Properties of the LiTFSI Doped N-Methyl-N-alkylpyrrolidinium⁺ TFSI Ionic Liquids, *J. Phys. Chem. B.* 110 (2006) 16879–16886. doi:10.1021/jp061930t.
- [181] S.-Y.Y. Lee et al., Two-cation competition in ionic-liquid-modified electrolytes for lithium ion batteries, *J. Phys. Chem. B.* 109 (2005) 13663–7. doi:10.1021/jp051974m.
- [182] M. Yamagata et al., Charge–discharge behavior of graphite negative electrodes in bis(fluorosulfonyl)imide-based ionic liquid and structural aspects of their electrode/electrolyte interfaces, *Electrochim. Acta.* 110 (2013) 181–190. doi:10.1016/j.electacta.2013.03.018.
- [183] S. Xiong et al., Analysis of the solid electrolyte interphase formed with an ionic liquid electrolyte for lithium-sulfur batteries, *J. Power Sources.* 252 (2014) 150–155. doi:10.1016/j.jpowsour.2013.11.119.
- [184] A.I. Bhatt et al., Application of the N-propyl-N-methyl-pyrrolidinium Bis(fluorosulfonyl)imide RTIL Containing Lithium Bis(fluorosulfonyl)imide in Ionic Liquid Based Lithium Batteries, *J. Electrochem. Soc.* 157 (2010) A66. doi:10.1149/1.3257978.

- [185] S. Fang et al., New functionalized ionic liquids based on pyrrolidinium and piperidinium cations with two ether groups as electrolytes for lithium battery, *J. Power Sources*. 196 (2011) 5637–5644. doi:10.1016/j.jpowsour.2011.02.047.
- [186] D.R. MacFarlane et al., Energy applications of ionic liquids, *Energy Environ. Sci.* 7 (2014) 232–250. doi:10.1039/c3ee42099j.
- [187] J.P. Salminen et al., Studies of Ionic Liquids in Lithium-Ion Battery Test Systems, *ECS Trans.* 1 (2006) 107–118. doi:10.1149/1.2209363.
- [188] C. Liu et al., Ionic liquid electrolyte of lithium bis(fluorosulfonyl)imide/N-methyl-N-propylpiperidinium bis(fluorosulfonyl)imide for Li/natural graphite cells: Effect of concentration of lithium salt on the physicochemical and electrochemical properties, *Electrochim. Acta.* 149 (2014) 370–385. doi:10.1016/j.electacta.2014.10.048.
- [189] H. Matsumoto et al., Fast cycling of Li/LiCoO₂ cell with low-viscosity ionic liquids based on bis(fluorosulfonyl)imide [FSI]⁻, *J. Power Sources*. 160 (2006) 1308–1313. doi:10.1016/j.jpowsour.2006.02.018.
- [190] T. Sugimoto et al., Ionic liquid electrolyte systems based on bis(fluorosulfonyl)imide for lithium-ion batteries, *J. Power Sources*. 189 (2009) 802–805. doi:10.1016/j.jpowsour.2008.07.053.
- [191] S. Seki et al., Compatibility of N-Methyl-N-propylpyrrolidinium Cation Room-Temperature Ionic Liquid Electrolytes and Graphite Electrodes, *J. Phys. Chem. C*. 112 (2008) 16708–16713. doi:10.1021/jp805403e.
- [192] J. Li et al., Improved electrochemical performance of LiMO₂ (M=Mn, Ni, Co)–Li₂MnO₃ cathode materials in ionic liquid-based electrolyte, *J. Power Sources*. 239 (2013) 490–495. doi:10.1016/j.jpowsour.2013.04.015.
- [193] R.S. Kühnel et al., Anodic stability of aluminum current collectors in an ionic liquid based on the (fluorosulfonyl)(trifluoromethanesulfonyl)imide anion and its implication on high voltage supercapacitors, *Electrochem. Commun.* 38 (2014) 117–119. doi:10.1016/j.elecom.2013.11.014.
- [194] K. Beltrop et al., Does Size really Matter? New Insights into the Intercalation Behavior of Anions into a Graphite-Based Positive Electrode for Dual-Ion Batteries, *Electrochim. Acta.* 209 (2016) 44–55. doi:10.1016/j.electacta.2016.05.012.
- [195] A. Moretti et al., Li-doped N-methoxyethyl-N-methylpyrrolidinium fluorosulfonyl-(trifluoromethanesulfonyl)imide as electrolyte for reliable lithium ion batteries, *J. Power Sources*. 269 (2014) 645–650. doi:10.1016/j.jpowsour.2014.06.170.
- [196] X. Lin et al., Thermally-responsive, nonflammable phosphonium ionic liquid electrolytes for lithium metal batteries: operating at 100 degrees Celsius, *Chem. Sci.* (2015) 6601–6606. doi:10.1039/C5SC01518A.
- [197] M.A. Navarra, Ionic liquids as safe electrolyte components for Li-metal and Li-ion batteries, *MRS Bull.* 38 (2013) 548–553. doi:10.1557/mrs.2013.152.

- [198] A. Guerfi et al., Improved electrolytes for Li-ion batteries: Mixtures of ionic liquid and organic electrolyte with enhanced safety and electrochemical performance, *J. Power Sources*. 195 (2010) 845–852. doi:10.1016/j.jpowsour.2009.08.056.
- [199] L. Aguilera et al., Enhanced low-temperature ionic conductivity via different Li^+ solvated clusters in organic solvent/ionic liquid mixed electrolytes, *Phys. Chem. Chem. Phys.* 18 (2016) 25458–25464. doi:10.1039/C6CP04766A.
- [200] D.M. and M.F. Paul M. Bayley, George Lane et al., Transport properties of ionic liquid electrolytes with organic diluents, *Phys. Chem. Chem. Phys.* 11 (2009) 7202–7208. doi:10.1039/b902200g.
- [201] S. Wilken et al., Ionic liquids in lithium battery electrolytes: Composition versus safety and physical properties, *J. Power Sources*. 275 (2015) 935–942. doi:10.1016/j.jpowsour.2014.11.071.
- [202] N. Pylahan et al., Ionic liquid and hybrid ionic liquid/organic electrolytes for high temperature lithium-ion battery application, *Electrochim. Acta*. 216 (2016) 24–34. doi:10.1016/j.electacta.2016.08.025.
- [203] N. Nishimura et al., 15Th Anniversary of Polymerised Ionic Liquids, *Polym. (United Kingdom)*. 55 (2014) 3289–3297. doi:10.1016/j.polymer.2014.02.042.
- [204] H. Ohno, Molten salt type polymer electrolytes, *Electrochim. Acta*. 46 (2001) 1407–1411. doi:10.1016/S0013-4686(00)00733-7.
- [205] M. Gouverneur et al., ^7Li nuclear magnetic resonance studies of dynamics in a ternary gel polymer electrolyte based on polymeric ionic liquids, *Electrochim. Acta*. 175 (2015) 35–41. doi:10.1016/j.electacta.2015.03.026.
- [206] G.B. Appetecchi et al., Ternary polymer electrolytes containing pyrrolidinium-based polymeric ionic liquids for lithium batteries, *J. Power Sources*. 195 (2010) 3668–3675. doi:10.1016/j.jpowsour.2009.11.146.
- [207] M. Safa et al., Polymeric Ionic Liquid Gel Electrolyte for Room Temperature Lithium Battery Applications, *Electrochim. Acta*. 213 (2016) 587–593. doi:10.1016/j.electacta.2016.07.118.
- [208] G.W.H. Höhne et al., *Differential Scanning Calorimetry*, Springer Berlin Heidelberg, Berlin, Heidelberg, 2003. doi:10.1007/978-3-662-06710-9.
- [209] P. Haines, *Principles of Thermal Analysis and Calorimetry*, Royal Society of Chemistry, Cambridge, 2002. doi:10.1039/9781847551764.
- [210] R.N.P. Choudhary et al., *Materials Science and Technologies : Dielectric Materials : Introduction, Research and Applications*, Nova Science Publishers, Inc., 2009.
- [211] K. Hayamizu et al., Ionic conduction and ion diffusion in binary room-temperature ionic liquids composed of EMIMBF₄ and LiBF₄, *J. Phys. Chem. B*. (2004) 19527–19532. <http://pubs.acs.org/doi/abs/10.1021/jp0476601>.
- [212] B. Schrader, ed., *Infrared and Raman Spectroscopy*, Wiley-VCH Verlag GmbH, Weinheim, Germany, 1995. doi:10.1002/9783527615438.

- [213] C. V. Raman et al., A New Type of Secondary Radiation, *Nature*. 121 (1928) 501–502. doi:10.1038/121501c0.
- [214] L.E. Barrosse-Antle et al., Voltammetry in room temperature ionic liquids: Comparisons and contrasts with conventional electrochemical solvents., *Chem. - An Asian J.* 5 (2010) 202–230. doi:10.1002/asia.200900191.
- [215] M. Hayyan et al., Investigating the electrochemical windows of ionic liquids, *J. Ind. Eng. Chem.* 19 (2013) 106–112. doi:10.1016/j.jiec.2012.07.011.
- [216] D. Pletcher, *A First Course in Electrode Processes*, 2nd ed., RSC Publishing, 2009.
- [217] A. Guerfi et al., Investigations on some electrochemical aspects of lithium-ion ionic liquid/gel polymer battery systems, *J. Solid State Electrochem.* 13 (2009) 1003–1014. doi:10.1007/s10008-008-0697-x.
- [218] B.A. Boukamp, A nonlinear least squares fit procedure for analysis of immittances data of electrochemical systems, *Solid State Ionics*. 20 (1986) 31–44. doi:10.1016/0167-2738(86)90031-7.
- [219] B.A. Boukamp, A package for impedance/admittance data analysis, *Solid State Ionics*. 18 & 19 (1986) 136–140.
- [220] A.J. Bard et al., *Electrochemical Methods*, 2nd ed., John Wiley & Sons, Inc., 2001.